ESTROGEN THERAPY IN A VIRAL MURINE MODEL OF MULTIPLE SCLEROSIS

A Thesis

by

FRANCISCO PASCUAL GOMEZ

Submitted to the Office of Graduate Studies of
Texas A&M University
in partial fulfillment of the requirements for the degree of

MASTER OF SCIENCE

August 2012

Major Subject: Biomedical Sciences

Estrogen Therapy in a Viral Murine Model of Multiple Sclerosis

ESTROGEN THERAPY IN A VIRAL MURINE MODEL OF MULTIPLE SCLEROSIS

A Thesis

by

FRANCISCO PASCUAL GOMEZ

Submitted to the Office of Graduate Studies of
Texas A&M University
in partial fulfillment of the requirements for the degree of

MASTER OF SCIENCE

Approved by:

Co-chairs of Committee,	C. Jane R. Welsh
	Jianrong Li
Committee Members,	Farida Sohrabji
	Ralph Storts
Head of Department,	Evelyn Tiffany-Castiglioni

August 2012

Major Subject: Biomedical Sciences

ABSTRACT

Estrogen Therapy in a Viral Murine Model of Multiple Sclerosis. (August 2012)
Francisco Pascual Gomez, B.S., Texas A&M University
Co-Chairs of Advisory Committee: Dr. C. Jane R. Welsh
Dr. Jianrong Li

Multiple sclerosis (MS) is an idiopathic neurodegenerative, demyelinating disease of the central nervous system (CNS). MS affects females more than males (3:1) and pregnancy reduces the number of relapses especially during the third trimester when 17-β-estradiol (E_2) and estriol (E_3) are at their highest levels. In order to study the role of estrogens as potential therapeutic agents for MS we investigated their role in Theiler's murine encephalomyelitis virus (TMEV)-induced demyelination (TVID).

SJL female mice were infected intracranially with Theiler's virus or PBS. The mice in the treatment groups were clinically scored and at week 20 they were ovarectomized (OVx) and given a subdermal pellet containing either 1) 0.1mg of E_2, 2) 5mg of E_3, or 3) placebo. Four weeks after treatment initiation, the mice were sacrificed and tissue samples were collected and vertebral columns and brains were fixed and placed in paraffin for histological analysis using either hematoxylin and eosin (H&E) stain for general anatomic features or Weil's stain for myelin.

No signs of clinical disease developed in any of the sham-infected mice. Prior to ovariectomy, infected mice had developed significant clinical scores indicative of demyelination. Mice in the placebo and E_3-treatment groups deteriorated rapidly whereas the E_2-treated mice improved significantly during the course of the treatment. Uteri were used to assess hormonal effects post-ovariectomy. Hormone treated groups were significantly different from placebo, indicating hormones were present. Hormone treatment showed significant differences among treatment groups for both inflammation and demyelination. E_2-treatment significantly decreased inflammation compared to placebo and E_3. E_2 was also effective in reducing demyelination compared to placebo

groups but not E_3. E_3 treatment was effective in reducing inflammation compared to placebo, but no significance was found for demyelination. Both E_3 and E_2 treated mice developed lower antibody levels against TMEV. The improvement in clinical signs, inflammation, demyelination, and the reduction of antibody levels in 17-β-estradiol-treated mice indicate a therapeutic potential for the treatment of MS.

DEDICATION

Para mi mamá, mi papá, y mi hermana. Gracias a su apoyo y su amor estoy donde estoy, son mi todo y este trabajo es prueba de que gracias a ustedes puedo hacer todo lo que me proponga.

Para mis abuelos Diego y Francisco y mis abuelas María Elena y Alicia, gracias por todo su apoyo incondicional

Para Isa, gracias por tu amor, paciencia y apoyo durante estos años.

To Dr. Jane Welsh for her patience, cheerfulness, and everything she helped me accomplish.

To the members of the Brazos Valley MS Support Groups for the idea to conduct this research project.

To the members of my committee and my professors for believing in me. Thank you for everything you taught me I take it to heart and I will never forget it.

“In every Triumph there’s a lot of Try”

“Your future depends on many things, but mostly you"

~Frank Tyger

『祝福(しゅくふく)の時(とき)は来(く)る、両手上(りょうてあ)げて』

(“A time for blessings will come, lift up both arms”)

ACKNOWLEDGEMENTS

First and foremost, I would like to say thank you the members of the Brazos Valley MS Support Group for their support and for giving us the idea behind this project; your questions and your support emails inspired us and let us know that together we can make a difference.

I would like to thank my committee for all their help in fulfilling this goal in my life. I am very fortunate to have met you and worked with you throughout this project: I would like to extend a very special thanks to Dr. Jane Welsh for allowing me to be a part of this project and for all the opportunities she gave me. Thank you for your support in every step of the way and providing me with the funding to carry out this project. I would like to thank Dr. Jianrong Li for all her input, her help, and her support and for her teachings, which allowed me to understand my project more in depth. I would also like to extend a very special thanks to Dr. Ralph Storts for his patience and for teaching me the basics of neuropathology I needed to carry out this project successfully. I would also like to say a big thank you to Dr. Farida Sohrabji for clarifying all the doubts on statistical methods and other questions as the project went along.

I wish to extend a very special thanks to Dr. Colin Young for his help in carrying out the Radio-Immuno Assays and his constant support throughout this project. Thanks to Lin Bustamante in the VIBS Histology Lab for her assistance in sectioning and staining the spinal cord sections used in this project. Thanks to Dr. John Roths for teaching me how to use the Vanox Microscope and allowing me to use it to capture the spinal cord sections.

Thanks to the undergraduate members of the Welsh-Young Lab for their assistance in this project. I would like to say thanks to Joy Cheng, Krystin Deason, Christina Dudash, Collin Mulcahy, Grace Philip, Ryan Trantham, Jake Wilkerson, and Jane Wang for assisting me in the various phases of this project

Special thanks are due to the Veterinary Integrative Biosciences Department at Texas A&M University and to Dr. Evelyn Tiffany-Castiglioni for the opportunity to be a

part of the department. I would like to thank to Dana Parks for always answering all my questions regarding departmental issues and teaching assistantship issues.

I would like to thank in a very special way Dr. Gregory Johnson, Dr. Gladys Ko, and Dr. Michelle Pine for believing in me and giving me the opportunity to assist them in their courses, to learn, to teach, and to be a positive impact on the lives of students. I also want to thank my professors in both my undergraduate and graduate careers for inspiring me with their enthusiasm and for their advice.

It is very important to me to say thanks to all my high school teachers. I know I was blessed to have such a great group of teachers at Central Catholic High School. They taught me to give my best, to always keep an open mind, to look forward and never look back, that hard work pays off, and most importantly they helped me discern my career goals as well as the pathway to reach them. I want to thank each and every one of them for the impact they had on my life.

Special thanks are due to Dr. Ildefonso Rodriguez Leyva and Dr. Jeronimo Rodriguez Rodriguez and the neurology residents at the Hospital Central "Dr. Ignacio Morones Prieto" for allowing me to experience medicine first-hand and for everything you taught me about neurology. Thank you for allowing me to see that the patient comes first and that we must do anything in our hands to make life better.

I would like to thank my friends for their support and for standing with me through it all. There is a saying that I like very much, "Chi trova un [vero] amico, trova un tesoro" ("Who finds a [true] friend, finds a treasure"), thanks to all of my friends I know this is true, and that I am blessed to have them in my life

Finally, I would like to say thanks to my mother, father, and sister for their love and encouragement, to my girlfriend for her patience, love, and encouragement, and to my grandparents and to my aunt Ana and uncle Héctor for their incomparable support.

NOMENCLATURE

MS	Multiple Sclerosis
RRMS	Relapsing-Remitting Multiple Sclerosis
PPMS	Primary Progressive Multiple Sclerosis
SPMS	Secondary Progressive Multiple Sclerosis
CNS	Central Nervous System
BBB	Blood-Brain Barrier
TMEV	Theiler's Murine Encephalomyelitis Virus
TVID	Theiler's Virus Induced Demyelination
L-protein	Leader Protein
EAE	Experimental Autoimmune Encephalomyelitis
MBP	Myelin Basic Protein
PLP	Proteolipid peptide
MOG	Myelin Oligodendrocyte Glycoprotein
pfu	Plaque forming units
OVx	Ovariectomy
E_2	17-β-estradiol
E_3	Estriol
ER	Estrogen Receptor
H&E	Hematoxylin and Eosin
RIA	Radio-Immuno Assay
mRNA	Messenger Ribonucleic Acid
Ab	Antibody
ITAbP	Intrathecal antibody production
Ag	Antigen
MHC	Major Histocompatibility Complex
HLA	Human Leukocyte Antigen
ANOVA	Analysis of Variance

DTH	Delayed-Type Hypersensitivity
CD	Cluster of differentiation
T_H	T-helper Cell
T_{CL}	Cytolytic T-cell
T_{Reg}	Regulatory T-cell
nT_{Reg}	Natural Regulatory T-cell
iT_{Reg}	Induced Regulatory T-cell
IL	Interleukin
SCID	Severe Combined Immunodeficient
pg	Picogram ($1x10^{-12}$ grams)
μg	Microgram ($1x10^{-6}$ grams)
mL	Milliliter ($1x10^{-3}$ liters)
NF-κB	Nuclear Factor-kappa B
PI3K	Phosphatidylinositol 3-kinase
TNF	Tumor Necrosis Factor
IFN	Interferon
MΦ	Macrophage
ASC	Antibody-secreting Cell
Ig	Immunoglobulin
TGF	Transforming Growth Factor
COX	Cyclooxygenase

TABLE OF CONTENTS

Page

LIST OF FIGURES

Page

LIST OF TABLES

Page

1. INTRODUCTION

Multiple sclerosis, (MS) is a chronic inflammatory, demyelinating, and neurodegenerative disease of the central nervous system (CNS). It can lead to severe disability in young adults, and, according to Gasperini *et al.*, it "is one of the most common causes of neurological disability in this population" (Gasperini *et al*., 2010). It affects young adults between 15 and 45 years of age, thus making it a high-impact neurological disease because of its effect on the working age group (Owens *et al*., 2011). It is thought that in MS, different components of the immune system recognize and attack myelin. These include, autoreactive T and B-cells, cytokines, macrophages (MΦ), and antibodies (Ab) directed against myelin. The loss of myelin and axonal damage lead to the characteristic progression of symptoms (Gasperini *et al*., 2010).

Multiple sclerosis also has more impact on Caucasians and females with a reported female to male ratio of 2:1 and in some places 3:1, and it tends to affect people living in temperate climates (Gold and Voskuhl, 2009). In the United States alone, MS affects more than a quarter million people. MS affects the central nervous system, thus its effects severely affect the individual's intellect as well as their ability to move and even their sight (Carlson, 2006).

1.1 Etiology

The etiology of MS is thought to be caused by autoimmune damage to myelinated axons followed by degeneration of the axons. As described by Encarta "[It] is chronic, unpredictable, and often progressive" and "[it] attacks and destroys tissues in the brain and spinal cord."(Carlson, 2006). There are four main types of MS. All forms affect nerve function, resulting in a variety of neurological manifestations. The most common type is the relapsing-remitting MS (RRMS). In this type, the patient has flare-ups and remissions –with periods where the patient does not show symptoms and

---

This thesis follows the style of the Journal of Neuroimmunology.

periods of pronounced disability. However, these patients do not deteriorate as fast as those with progressive MS. After a period of 10 years or more, 50% of MS patients may exhibit the Secondary-Progressive phase, which is like RRMS, but with increasing deterioration. Another type of MS that is not as common is Primary-Progressive MS (PPMS). In this form the patient just deteriorates steadily from the onset of the disease without any flare-ups and remissions. The rarest form of MS is the Progressive-Relapsing form, which causes the worst symptoms in the shortest period of time. Although patients will have remissions, when the symptoms return they are more severe and the flare-ups experienced become increasingly worse (Carlson, 2006).

There are several schools of thought that address the possible etiology of MS. The most accepted theory is that in MS the immune system has a misdirected response against the myelin sheaths resulting in damage to the axons, which "leads to permanent loss of neurological function" (Gasperini *et al*., 2010). Myelin acts as an insulator to aid nerve impulses travel at velocities required to accurately relay information. When the immune system disrupts this myelin sheathing, the speed of transmission decreases or is completely interrupted. The neurological effects vary depending on the nerve affected. If the damage is in the pathway supplying the muscles it causes muscular problems, if on a sensory pathway, it may cause the loss of a sense, such as eyesight (Carlson, 2006).

A proposed mechanism for the immunopathogenesis of MS involves activation of autoreactive T-cells by an unknown factor. It has been proposed that molecular mimicry or bystander activation may be one of the factors leading to activation. Once activated, the T-cells can cross the blood-brain barrier (BBB) and possibly lead to its degradation. Once in the CNS, the cells can interact with Mϕ, B-cells, or microglia and lead to the release of pro-inflammatory cytokines. Plasma cells can also migrate into the brain via a disrupted BBB and secrete antibodies against myelin proteins. This causes the degradation of the myelin sheath, recruitment of more inflammatory cells, and the release of free radicals, nitric oxide (NO), and proteases by local microglia. These events eventually culminate in tissue damage and axonal loss leading to the onset of symptoms (Gold and Wolinsky, 2011)

Genetics also plays a role in the susceptibility to MS with an increase in the incidence in patients that have the HLA-DR2 genes of the major histocompatibility complex (MHC) Class II (Gold and Wolinsky, 2011). In addition, the interleukin 2 receptor (*IL-2RA*/CD25) and interleukin 7 receptor (*IL-7RA*/CD127) genes have been identified as possible genetic components for MS (Gold and Wolinsky, 2011; Libbey and Fujinami, 2010; Olsson and Hillert, 2008). These findings give support to the autoimmune hypothesis, as MHC genes are involved in antigen presentation and certain alleles may predispose to reactions against self, or specifically against self-myelin.

Infectious agents, viruses or bacteria, have also been implicated in the pathogenesis of MS. Viruses implicated as "suspect agents" that could trigger MS include: Epstein-Barr virus, *Herpes simplex* virus, *Varicella zooster* virus, Cytomegalovirus, *Herpes hominis* type-6 (Human Herpes Virus 6), measles virus, human T-cell lymphotrophic virus, or an endogenous retrovirus known as Human Endogenous Retrovirus (HERV) (Goodin, 2009; Libbey and Fujinami, 2010; Miller *et al*., 2001; Sato *et al*., 2011). Other evidence that favors a viral etiology include the following criteria according to Libbey and Fujinami (Libbey and Fujinami, 2010): 1) Characterization of MS lesions demonstrates $CD8^+$ T-cells in infiltrates. The $CD8^+$ T-cells function in cell-mediated immunity to protect against viral infections; 2) Relapses in MS correlate with increases in viral titers during infection; 3) Antibodies against the various viruses mentioned previously have been detected in MS patients; 4) Peripheral infection can create molecular mimicry that can cause autoimmune reactions. When we consider all these possibilities and the fact that there has not been a clear association between the above viruses and MS patients, it becomes clear that isolating a single causal agent is improbable, especially in the case of mimicry (Libbey and Fujinami, 2010).

Another mechanism, proposed to explain the pathogenesis of MS, hypothesizes that the disease arises as a result of viral infection combined with an overactive immune system which attacks myelin in genetically susceptible individuals. The infectious agent may also mimic host proteins, thus the immune system reacts and attacks both the

pathogen and host tissues (Carlson, 2006). This hypothesis may also explain the relapsing-remitting characteristic progression of the disease as well as other forms of disease progression. Epstein-Barr virus (EBV) infection has been implicated in other autoimmune disorders as well as in MS, including Sjorgen's syndrome, rheumatoid arthritis, and systemic lupus erythematosus. In addition, some reports have found viral titers of EBV in MS brains and the diseases mentioned above (Goodin, 2009). Human Herpes Virus type 6 (HHV6) has also been found in MS lesions (Miller *et al*., 2001). However, there is an important point to be made in that many of the viruses isolated on MS brains have also been found in normal brains or have not been consistently detected in MS brains. Therefore, the etiology of MS may not be due to a single infectious agent but rather a variety of organisms.

A new hypothesis that was proposed by Stadelmann *et al.*, suggests that the symptoms of MS may not only be due to demyelination. The neuro-axonal damage may also be due to a neurodegenerative component. This emerged as a result of evidence from cortical observations of different types of brain lesions in MS patients (Stadelmann *et al*., 2008). These cortical lesions, according to Calabrese *et al.*, show less inflammation but do have demyelination, axonal loss and neuronal apoptosis, or cell death (Calabrese *et al*., 2008). Both studies agree that perhaps it is these cortical lesions that cause some of the more severe neurological manifestations of MS (Calabrese *et al*., 2008; Stadelmann *et al*., 2008). The Stadelmann study, however, does recommend that these results be retested using more modern imaging techniques in order to obtain better data (Stadelmann *et al*., 2008).

1.2 Main Basis for This Research Project

Evidence for the autoimmune etiology of MS comes from its preference for the female sex. The most widely recognized autoimmune disorders that shows the strongest female prevalence is Sjörgen´s syndrome with a 95% incidence rate in females followed closely by systemic lupus erythematosus (SLE) at 90% incidence, and Multiple Sclerosis is in sixth place with an approximately 60% incidence rate (Whitacre, 2001). There is

also a marked difference in how these diseases present in males and females and there is also sexual dimorphism in the immune response. In a recent study by Smith-Bouvier *et al.*, a novel model of mice was used to show if chromosomal gender had an impact in susceptibility to autoimmune disease. The group tested this hypothesis using XX and *Sry*-deficient XY^- female mice and XX*Sry* and XY^-*Sry* male mice that were gonadectomized to examine the effects of chromosome complement without any sex hormones (Smith-Bouvier *et al*., 2008). They found that XX sex chromosome complement makes SJL mice more susceptible to both experimental autoimmune encephalomyelitis (EAE) and the pristane-induced lupus model (Smith-Bouvier *et al.*, 2008). In addition, the immune response is altered by XX complement, with XY^- females producing anti-inflammatory T_H2 cytokines such as IL-13 and IL-5 (Smith-Bouvier *et al*., 2008). This may help explain why females may be more susceptible to autoimmune diseases, and why they are more often afflicted with MS.

In animal models, females produce more antibodies and their T-cell activation is more robust. However, in human studies the only noticeable difference is that females have an increased absolute number of $CD4^+$ lymphocytes but not necessarily increased levels of antibody or cytokines (Whitacre, 2001). Female hormones modulate the immune response and have been shown to dampen the T_H1 response commonly seen in autoimmune disorders during pregnancy (Voskuhl, 2003; Whitacre, 2001). Males seem to have a higher prevalence of primary progressive Multiple Sclerosis (PPMS), especially when they are younger than 30 years of age with the male-to-female ratio of 1:1 (Cottrell *et al*., 1999). As patients with this rare form of MS age, the ratio begins to switch to the traditional 1:2 seen in relapsing-remitting MS (RRMS) which may indicate a relationship with sex hormones: as female hormones decline with menopause the ratio seems to favor men whose testosterone levels remain into later decades of life (Cottrell *et al*., 1999). Testosterone has been shown to have a protective role by causing a shift toward a T_H2 (antibody-mediated or humoral immunity) response that reduces the effect of autoimmune disorders, which are primarily T_H1 (cell-mediated immunity) responses, and both testosterone and estrogens have been shown to have neuroprotective roles

(Gold and Voskuhl, 2009). These observations prompted us to further investigate the relationship between sex hormones and the susceptibility of women to MS and the onset and severity of symptoms.

The principal hormones that are addressed by this research project are the estrogens; namely, 17-β-estradiol (E_2) and estriol (E_3). These compounds are similar, with estriol having an extra hydroxyl (-OH) group. However, functionally these hormones perform totally different tasks. E_3 is a hormone that increases to high levels during pregnancy. It is commonly referred to as a hormone of late pregnancy since it is produced by the fetal-placental unit (Sicotte *et al*., 2002). In contrast, E_2 plays several roles in the body and it can be found in both males and females with females having much higher concentrations. In the Pregnancy in Multiple Sclerosis (PRIMS) European multicenter study, pregnant women with MS were recruited in between January 1993 and July 1995. A total of 254 pregnant women responded to the study and the average relapses were obtained three months before pregnancy, during pregnancy, and three months after. Pregnancy has been shown to decrease the relapse rate especially during the third trimester, coinciding with the highest levels of estrogens and then increases markedly upon delivery as levels of estrogens fall (Abramsky, 1994; Confavreux *et al*., 1998; Gold and Voskuhl, 2009; Rinta *et al*., 2010; Stuart and Bergstrom, 2011).

Pregnancy seems to have an effect on the immune system shifting responses from T_H1 to T_H2 and in the case of diseases like MS, this setup could explain the marked decrease in the relapse rate (Confavreux *et al*., 1998). These observations have also been made when comparing pre-menopausal and post-menopausal patients noting that as endogenous estrogen levels wane in post-menopausal patients, the relapse rate increases (Smith and Studd, 1992). Clinical trials reported by Sicotte *et al.* and by Soldan *et al.* have shown estriol treatment in human patients as a promising treatment option for MS and suggests that hormones may indeed be playing a role in disease modulation in patients with MS (Sicotte *et al*., 2002; Soldan *et al*., 2003). In addition, hormonal therapy with oral contraceptives (OC) has shown a decrease in the number of relapses (Stuart and Bergstrom, 2011), the severity of symptoms, and the incidence of MS in OC

users was reported as 40% lower if the drugs used contained ethinyl estradiol and a progestagen when compared to non-users (Alonso *et al.*, 2005; Nicot, 2009). Progesterone treatments in nonovariectomized experimental autoimmune encephalomyelitis (EAE) C57Bl/6 mouse models have shown that treatment with 100mg pellets give levels of progesterone comparable to pregnancy (~75ng/mL) and lead to an attenuation of symptoms and increased levels of protective cytokines, such as interleukin-10 (IL-10) (Garay *et al*., 2007; Yates *et al*., 2010). However, we will focus solely on the effects of estrogens as a means to observe hormonal effects on a viral model of MS.

1.3 Theiler's Murine Encephalomyelitis Virus (TMEV) Model

Researchers have used two murine – mouse – models in the majority of research related to MS, and each uses different approaches to establish the disease. The first model, which will not be addressed by this project, is the Experimental Autoimmune Encephalomyelitis (EAE) model. This model uses injections of myelin proteins with an adjuvant to cause an autoimmune attack on myelin. This is a purely non-infectious model that focuses exclusively on the autoimmune aspect of MS. To induce EAE, mice are inoculated with a myelin peptide, either Myelin Basic Protein (MBP) or proteolipid peptide (PLP), in complete Freund's Adjuvant (CFA) containing *Mycobacterium tuberculosis*, and induced via injection with pertussis toxin (Bebo *et al*., 2001).

This project utilizes the Theiler's murine encephalomyelitis virus (TMEV), which causes Theiler's virus-induced demyelination (TVID) in susceptible mice strains. TMEV is a non-enveloped, positive sense, single stranded RNA virus belonging to the genus *Cardiovirus*, in the family *Picornaviridae* (Sato *et al*., 2011). TMEV has been divided into two subgroups: GDVII and Theiler's original (TO). The Theiler's original strains cause a persistent infection of the CNS in susceptible strains of mice, followed by demyelination whereas the GDVII strains cause lethal encephalitis is all strains of mice. This project will use SJL/J female mice since this strain is highly susceptible to developing a persistent demyelinating infection of the CNS.

The choice of model relates back to the proposed post-viral autoimmune etiology hypothesis. The TMEV model offers several similarities to human MS: First, it is a chronic inflammatory disease of the white matter with gray matter involvement; second, symptoms are caused by myelin breakdown, which is in turn mediated by a T_H1 response (mainly $CD4^+$ cells); and third, mice develop autoimmune responses. In addition, disease can be spontaneously induced in mouse colonies because Theiler's is a natural pathogen of mice (Miller *et al*., 2001). The most virulent groups of Theiler's virus are the FA and GD-VII groups and they cause a fatal disease in mice known as acute polioencephalomyelitis (Oleszak *et al*., 2004; Roos, 2010). The onset of disease post-infection with either of the less virulent members of the Theiler's Original (TO) group, the Daniels (DA) or the "tissue culture-adapted BeAn strain" is usually characterized by infection of the gray matter, especially motor neurons, leading to a poliomyelitis that may or may not be fatal (Miller *et al*., 2001; Sato *et al*., 2011). The mice that survive this period, develop a "chronic, progressive, inflammatory demyelinating disease" that persists primarily in the spinal cord (Miller *et al*., 2001; Roos, 2010). Like MS, the exact defined mechanism for demyelination induced by TMEV is unclear. Demyelination may arise as a result of either direct lysis of infected oligodendrocytes by the virus or by the immune system, or lysis of uninfected oligodendrocytes by an over-reactive immune system or via bystander responses (Libbey and Fujinami, 2010). Comparable to progressive MS there is no clear gender bias with the Theiler's virus model. However, in other strains such as the C57L/J, the opposite gender bias exists with males being severely affected and females showing more resistance (Fuller *et al*., 2005; Kappel *et al*., 1990). All these characteristics make the Theiler's murine encephalomyelitis virus-induced demyelination (TMEV-ID) model, ideal to study the effect of hormones on MS. In this model, H&E stains characteristically show lymphocytic infiltrates in the parenchyma and around blood vessels (perivascular cuffing), meningitis, and status spongiosus. The lack of uptake of the Weil's stain for myelin emphasizes areas of demyelination. The demyelinating lesions seen in TVID are very similar to those seen in human MS. In addition, there was a recent discovery of a

cardiovirus related to TMEV that can infect humans, the Saffold virus (Chastain *et al*., 2011; Roos, 2010). Thus the TMEV model may prove to be important to determine the mechanisms of MS pathogenesis.

The main goal of this study was to determine the effectiveness of E_2 and E_3 as therapeutic agents for the treatment of (TMEV)-induced demyelination (TVID). We hypothesize that the immune modulatory properties of these two hormones will cause a decrease in clinical signs of disease and also decrease inflammation and consequently demyelination and neurodegeneration in the spinal cords of TMEV infected mice.

2. MATERIALS AND METHODS

2.1 Project Design

The project was divided into two main parts: Development of demyelinating disease as a result of infection and then hormone treatment. Figure 2.1 is a project timeline showing the events that took place from infection to termination. Table 2.1 shows the project design and distribution of mice into groups. Originally eight (8) mice were assigned to each group. During the course of the experiment, two mice were lost in the TMEV-infected placebo treatment group. One mouse from each of the hormone treated uninfected groups died.

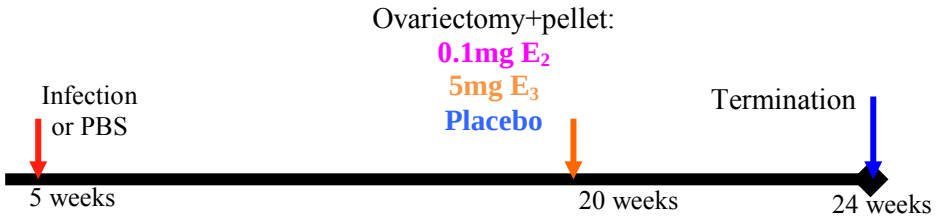

Figure 2.1 Project timeline from infection to termination.

Table 2.1 Project design.
Group distributions for each treatment option

17-β-estradiol (E_2) (0.1 mg) treatment	Estriol (E_3) (5 mg) treatment	Placebo treatment (Control)
n=7 - Non-infected (PBS)	n=7 - Non-infected (PBS)	n=8 - Non-infected (PBS)
n=8 - TMEV Infected	n=8 - TMEV Infected	n=6 - TMEV Infected

2.2 Subjects

Groups of four female SJL mice (Jackson Labs) were assigned to twelve different cages (N_{Total}=48). The mice had access to food and water *ad libitum.* For this experiments six different experimental groups were created: three groups were infected with virus at 5 weeks of age and three groups were used as age-matched sham-infected controls. At 20 weeks of age (15 weeks post infection), all mice were ovariectomized (OVx) and then given either: a 0.1mg 17-β-estradiol (E_2) pellet, a 5mg estriol (E_3) pellet, or a placebo pellet placed subdermally (Bebo *et al*., 2001; Palaszynski *et al*., 2004; Wang *et al*., 2009). All animals were housed and handled in accordance with the Texas A&M University Institutional Animal Care and Use Committee (SACC) (AUP# 2007-218, 2007-2010).

2.3 Virus and Infection

For this project, we utilized the BeAn strain of Theiler's virus (obtained from Dr. H.L. Lipton, Department of Neurology, Northwestern University, Chicago, IL). The virus was previously propagated and amplified in BHK-21 cells and the culture supernatant was stored at -70ºC (Welsh *et al*., 1987).

At 5 weeks of age, 24 mice (n=24) were anesthetized with isoflurane and infected intracranially into the right cerebral cortex with 5 x 10^4 plaque forming units/mL (pfu/mL) of the BeAn strain of TMEV. Controls (n=24) were given a similar injection with Phosphate Buffered Saline (PBS) intracranial injection into the right cerebral cortex

2.4 Behavioral Measurements – Clinical Symptoms

All mice were evaluated for clinical signs of disease weekly. This project focused on behavioral evaluations during the chronic phase of TMEV infection, paying close attention to trends in improvement after ovariectomy and treatment. We utilized a scoring system based on Borrow *et al*, 1998 and Sieve *et al*. (2004). The scoring system provides a range of values from 1 to 6. The scores were given as follows

1=some weakness in the hind limbs,

2=slight wobble,

3=wobbly gait,

4=pronounced wobbly gait, loss of righting reflex, mice hunch or arch their backs,

5=incontinence in addition to symptoms in 4, and

6=moribund mice (Sieve *et al*., 2004).

The data was obtained, averaged and plotted as a score vs time chart using Microsoft Excel.

2.5 Tissue Samples and Preparation

All mice were euthanized at 19 weeks p.i., which represents the 24th week of the experiment. The mice were perfused via the left ventricle with PBS followed by 10% formalin in phosphate buffer pH 7.2. The uteri, spleens, brains, and vertebral columns were collected. Uteri were weighed to assess exogenous hormonal effects on the mice and discarded after their weight was recorded. The spleens were flash frozen in liquid nitrogen and stored at -80ºC. The brains and spinal cords were dehydrated and embedded in paraffin blocks. They were stored at 4ºC until they were sectioned and stained (Campbell *et al*., 2001).

The present study focused on lesions in the spinal cord since previous research has shown that the spinal cord is regularly affected during the chronic phase of the TMEV infection (Blakemore *et al*., 1988; Young *et al*., 2010). Vertebral columns containing intact spinal cord were removed and sectioned transversely into 12 pieces. Spinal cords were serial sectioned on a microtome at either 5µm for Hematoxylin and Eosin (H&E) staining or at 10µm for Weil's staining. They were mounted on individual slides containing 12 sections per animal and covering cervical, thoracic, lumbar, and sacral/*conus medullaris* divisions of the spinal cord.

2.6 Light Microscopy and Image Captures

An Olympus VANOX AHBS3 microscope with an adapted digital camera was used for all image captures. Hematoxylin and Eosin (H&E) slides were captured at 40x magnification using a SPOT Insight QE digital camera (Diagnostic Instruments, Inc). Due to a software update and the purchase of a new camera, the Weil's-stained slides were captured at 40x magnification using an SPOT RT Slider digital camera (Diagnostic Instruments, Inc). Both cameras had a 1.0x magnification. The software used for image capturing was SPOT Software version 4.6 (Imaging Solutions division of Diagnostic Instruments, Inc.)

2.7 Hematoxylin and Eosin (H&E) Staining and Lesion Evaluation

Sections of the paraffin-embedded vertebral column were cut at 5µm and then stained with H&E by Lin Bustamante at the Veterinary Integrative Biosciences (VIBS) Histotechnology Lab according to their established Hematoxylin and Eosin (H&E) staining protocol presented here:

> The sections were deparaffinized with three series of 15-20 dips each in Pro-Par Clearant and rehydrated in two 10-15 dips in 100% ethanol (EtOH). The sections were then dipped for two series of 10-15 times each in 95% EtOH and then in one series of 10-15 dips in 70% EtOH. The sections were washed three times with distilled water. The sections were stained in Hematoxylin 560 (Surgipath cat # 01571/Leica Microsystems cat # 3801571) for 4 minutes. Afterwards they were washed in tap water until clear. The slides then underwent a series of 2-3 quick dips in a solution made up of 1% hydrochloric acid (HCl) and 70% EtOH (0.5% acid alcohol) to differentiate them. The sections were rinsed with tap water three times and were dipped 2-3 times in a 0.5% lithium carbonate (Li_2CO_3) solution (1.54g Li_2CO_3 in 100mL distilled H_2O) to give them a blue tint. Once the sections are stained blue, they are washed in running tap water four times and rinsed with 10-15dips in 80% EtOH. The sections can then be counterstained in 0.5% Alcoholic Eosin Y (StatLab, cat# SL98-1) in a series of 1-10 dips. The

sections are dehydrated using two series of 3-5 dips in 95% EtOH and three series of 10-20 dips in absolute EtOH. The stain was finalized by clearing using 10-15 dips in xylene and then four series of 10-15 dips in Pro-Par Clearant. The slides were then mounted and cover-slipped.

The TMEV model is characterized by inflammatory lesions of the spinal cord, and previous studies have shown restraint stress alters the immune systems response to TMEV in these areas using a categorical system of measurement based on lesion expression (Campbell *et al*., 2001; Sieve *et al*., 2006; Sieve *et al*., 2004). This project utilized area measurements to determine percent inflammation in the different spinal cord segments evaluated making the results more quantitative and facilitating interpretation (Campbell *et al*., 2001; Meagher *et al*., 2007; Sieve *et al*., 2004).

Independent raters blind to the subjects' treatment and condition were assigned different groups of mice and were asked to measure perivascular cuffing (perivascular accumulation of lymphocytes and macrophages) using ImageJ Software (National Institutes of Health). S*tatus spongiosus* (where possible demyelination could occur) were noted on the sections. All divisions of the spinal cord were measured on the slides – with the exception of the *conus medullaris* – at 40x magnification.

The three measurements obtained from each section were: Total cord area, gray matter area, and area of inflammation (sum of areas, including cuffing and parenchymal) if applicable. White matter area was obtained using the equation: [Total cord area (pix^2)]-[Gray matter area (pix^2)]. Percent white matter inflammation was obtained by the equation: [Area of inflammation (pix^2)]/[Total white matter area (pix^2)]x100. The author supervised the raters and their data was checked for accuracy. Data was recorded on Microsoft Excel software. Analyses of the inflammatory lesions of the spinal cord were conducted for comparison of the percent parenchymal inflammation among groups.

2.8 Weil's Staining and Lesion Evaluation

Demyelination was evaluated following staining of serial sections with the Weil's method for myelin. The Weil's stain uses iron alum and hematoxylin to visualize areas

with diminished myelin, or lipid-rich contents (Young *et al*., 2010). Sectioning (10μm) and staining were done by Lin Bustamante at the VIBS Histotechnology lab according to a modified protocol based on Arthur Weil's original method (Weil, 1928):

> A stock solution of Weil's solution is prepared by mixing 45mL of 4% ferric alum ($FeNH_4(SO_4)_2$-$12H_2O$) with 5mL of 1% stock hematoxylin solution. A solution of Weigert's Borax ferricyanide solution is prepared by mixing 2g Borax (Sodium borate [$Na_2B_4O_7$-$10H_2O$]), 2.5g potassium ferricyanate ($K_3Fe(CN)_6$) in 200mL of distilled H_2O. A 0.5% solution of Lithium carbonate (Li_2CO_3) is prepared by mixing 0.5g Li_2CO_3 with 100mL distilled H_2O.
>
> The sections were deparaffinized in absolute EtOH and placed in 0.5% celloidin for 10 minutes to prevent detachment from the slide, and were left to air dry for 15 minutes. The slides were then placed in 70% EtOH for 5 minutes and then washed with distilled H_2O. The slides were then placed in prepared Weil's solution for 10-45 minutes at 50-60ºC. After that period of time, the slides are washed with tap water. Using the microscope, the slides are placed back in the Weil's solution and checked for differentiation of white matter or areas of degeneration. Once the desired level is reached, the slides are washed with distilled H_2O (several changes). To complete the differentiation, the slides are placed in the Weigert's borax ferricyanide solution and checked under the microscope. Once the white matter/lesion areas are differentiated, the slides are again washed in several changed of distilled H_2O, and then in tap water. The slides are placed in the Li_2CO_3 solution for one minute and then rinsed in sequence with tap and distilled H_2O respectively. The slides are then dehydrated in EtOH, cleared in xylene and mounted and cover-slipped.

Independent raters blind to the subjects' treatment and condition used ImageJ Software (National Institutes of Health) to separately identify and outline areas of demyelination for each group assigned. All divisions of the spinal cord were measured on the slides – with the exception of the *conus medullaris* – at 40x magnification.

Once again, the three measurements obtained from each section were: Total cord area, gray matter area, and area of demyelination (sum of areas) if applicable. Each measurement was repeated twice and the values averaged. Average White matter area was obtained using the equation: [Average Total cord area (pix^2)]-[Average Gray matter area (pix^2)]. Percent white matter demyelination was obtained by the equation: [Average Area of demyelination (pix^2)]/[Average Total white matter area (pix^2)]x100. The average values were used for all analyses of the demyelinating lesions of the spinal cord. Statistical analyses were conducted for the percent parenchymal demyelination. Data was recorded on Microsoft Excel software.

2.9 Theiler's Virus Antibody (Ab) Levels

Radio-Immuno Assays (RIAs) using Theiler's virus (GD-VII) as antigen (Ag) were performed using the sera collected from each mouse at termination according to the protocol described by Sieve *et al*. (2004). Flexible U-shaped, 96-well polyvinyl chloride plates (Costar, Cambridge, MA) were rinsed five times with Tween 20 (0.05%v/v) in Reverse Osmosis water (RO-H_2O) and then rinsed five times with RO-H_2O. The wells were then blot dried and 1µg/well of the Theiler's virus antigen (GD-VII, $1.0x10^{-7}$ pfu/100µL) in carbonate buffer (pH=9.6) was added to coat the bottom of the wells. To block the plate, 100µL of a buffer made of 495mL of a solution made from 0.08M Trizma HCl, 0.03M Trizma base, and 0.15M NaCl (final pH of 7.2), and 5mL of a solution made from 1.0% nonfat dry milk (NFDM) and 0.5% Tween-20 in RO-H_2O. The plates were incubated for 24h at 4ºC. The plates were washed with Tween 20 (0.05%v/v) in Reverse Osmosis water (RO-H_2O) and rinsed with RO-H_2O once again and blocked with 3.0% NFDM in phosphate buffered saline (PBS, pH 9.0) using 200µL/well. The plates were incubated at 37ºC for 1h. After washing and blot drying, 10µL of mouse sera were added to the plates and diluted in 190µL of PBS containing 0.1% Bovine Serum Albumin (BSA) and NaN_3 to create a 1/20 dilution. Serial dilutions were then made by taking 100µL of the 1/20 dilution, adding it to 100µL of PBS and mixing. The dilutions made were 1/40, 1/80, 1/160, 1/320, and 1/640. At the end, 100µL of the 1/640 dilution

were discarded to keep a 100µL volume per well. The plates were then incubated for 1h at 37ºC and washed as described above. Following the wash, 100µL of rabbit anti-mouse IgG diluted 1/500 from stock *(*Accurate Chemical and Scientific, New York*)* were added to each well. The incubation and washing was repeated, and then 100µL of Protein-A-I^{125} ($1x10^5$ counts per minute [CPM]) were added to the wells and incubated at room temperature for 1h. After rinsing, the wells were cut and placed in tubes and radioactice counts read using a micromedic 4/200 plus automatic gamma counter (Sieve *et al*., 2004).

The results were transposed to Microsoft Excel and CPM to dilution charts were made for uninfected and infected mice and the respective treatment groups.

2.10 Statistical Analysis

The data is presented as Mean ± SEM. Data for behavioral/clinical scores was analyzed with Prism Software (GraphPad Software, Inc.) using the non-parametric Kruskal-Wallis test with Dunn's Multiple comparison *post hoc* test. Data for uterine weights, spleen weights, and radio-immuno assays (RIAs) was analyzed with SPSS Statistics 20 (IBM) using a Two-way Analysis of Variance (2-way ANOVA) with a Least Squares Difference (LSD) *post hoc* test. Data for percent inflammation and percent demyelination, and comparison of the infected treatment groups in the RIAs was analyzed using a One-Way Analysis of Variance (1-way ANOVA) with a Least Squares Difference (LSD) *post hoc* test. For all data analyzed, statistical significance was achieved if $p<0.05$.

3. RESULTS

3.1 Estradiol (E_2)-treatment Ameliorates Clinical Signs of Disease

Mice were evaluated once weekly for signs of disease and data is shown for scores beginning at week 17 post-infection (pi) in order to evaluate the chronic phase of TMEV infection. Scores for the weeks post treatment (Weeks 21-24) were averaged and evaluated for an effect of treatment on clinical symptoms of disease. Table 3.1 shows the mean weekly scores per treatment group and the overall mean score for the four-week treatment period. The overall mean clinical score for the placebo treated mice was 3.8616 $\pm$0.1057; whereas E_2 treated mice scored 3.3750 $\pm$0.0846 and for E_3 treated mice 3.6719 $\pm$0.0771. Figure 3.1 is a graphical representation of the mean scores. Non-parametric Kruskal-Wallis analysis showed a significant difference among the all three groups for the mean weekly scores ($H_{(2)}$: 6.865, p<0.05). The scores began to diverge and become significantly different among the three groups at weeks 23 ($H_{(2)}$: 7.337, p<0.05) and 24 ($H_{(2)}$: 10.39, p<0.05). The Dunn's Multiple comparison *post hoc* test showed that E_2 treatment significantly decreased clinical scores compared to placebo treatments at ameliorating scores post ovariectomy (p<0.05) but scores were not different from E_3-treatment groups (p>0.05). There was no difference between placebo-treated groups and E_3-treated groups (p>0.05). Regression lines were fitted to each plot revealed that both placebo and E_3-treated groups tend to increase in score severity as indicated by their positive slopes (m), while the E_2-treated group seems to ameliorate based on its negative slope (m); however, the R^2-value (R^2=0.082) for the E_2 regression line is not high enough to claim this effect.

Table 3.1 Mean weekly clinical scores.
The mean clinical scores per experimental group are presented in this table in addition to the overall averages for the four-week treatment period

	Week	Placebo Tx n=6	E_2 Tx n=8	E_3 Tx n=8
Avg	21	3.7500	3.3125	3.5938
SEM		0.0945	0.1619	0.2001
Avg	22	3.6429	3.6250	3.5000
SEM		0.1429	0.1250	0.1637
Avg	23	3.9286	3.2500	3.7500
SEM		0.1304	0.1336	0.2113
Avg	24 (term.)	4.1250	3.3125	3.8438
SEM		0.1548	0.1315	0.1151
	Overall Average	3.8616	3.3750	3.6719
	SEM	0.1057	0.0846	0.0771

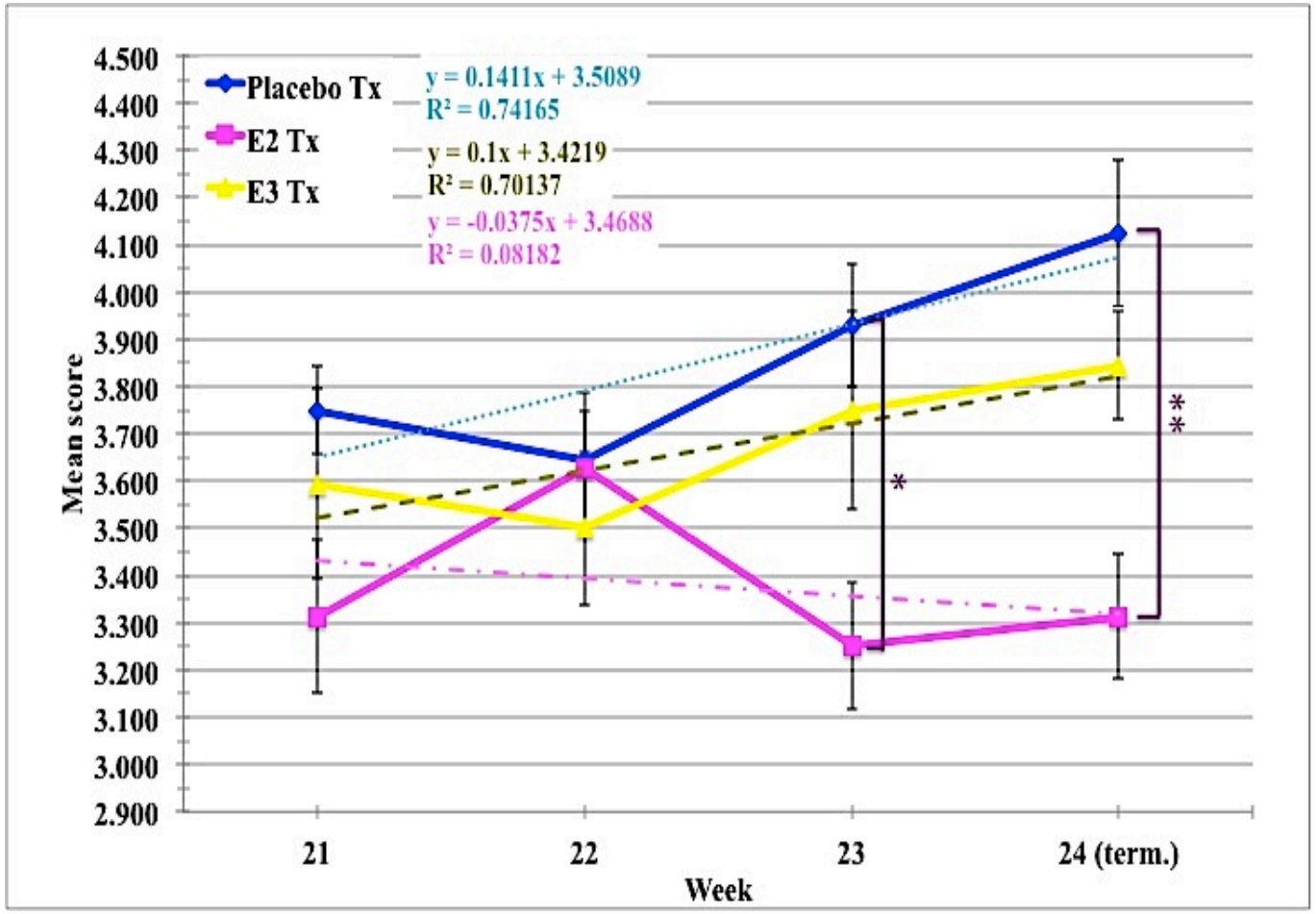

Figure 3.1 E_2-treatment ameliorates the mean clinical scores when compared to placebo treatment.
Scores following ovariectomy were significantly different among treatment groups ($p<0.05$). Hormone treatment with E2 began showing a marked effect compared to placebo.

3.1.1 Before-and-After Clinical Score Comparison Showed Both E_2 and E_3 Treatment Groups Exhibit Similar Rates of Disease Progression, but E_2-treatment Maintained Lower Clinical Scores

Table 3.2 shows the mean before and after scores per group comparing week 17, when we began measuring scores, to week 24 (termination). Figure 3.2 depicts this data graphically for the different treatment groups between week 17 and week 24 post-infection. Regression lines fitted to the plots showed that all scores had a tendency to increase. Treatment with E_2 had the same increase in score as E_3 as indicated by the slope (m) of their respective regression lines (m=0.5938) and placebo-treatment showed the steepest increase in score (m=1.1875). Non-parametric Kruskal-Wallis analysis was used to compare the three groups at week 17 and week 24, respectively. No significant difference was found among groups during week 17 ($H_{(2)}$: 3.572; p>0.05); however, the group scores were significantly different at termination ($H_{(2)}$: 10.39; p<0.05). Though E_2-treatment increased at the same rate as E_3, the range of scores remained lower than E_3. The final score of E_2 treatment was significantly different from placebo (p<0.05) but not from E_3-treated groups. There was no significant difference between E_2 and E_3 treatment groups (p>0.05).

Table 3.2 Mean clinical scores from week 17 and week 24.
Mean clinical scores for both endpoints per group with the standard error are presented in this table. The average score per group is also shown

	Week	**Placebo n=6**	**E_2-Tx n=8**	**E_3-Tx n=8**
Avg	17	2.93750	2.71875	3.25000
SEM		0.14752	0.26490	0.16366
Avg	24 (term.)	4.12500	3.31250	3.84375
SEM		0.15478	0.13153	0.11512
	Average	3.53125	3.01563	3.54688
	SEM	0.59375	0.29688	0.29688

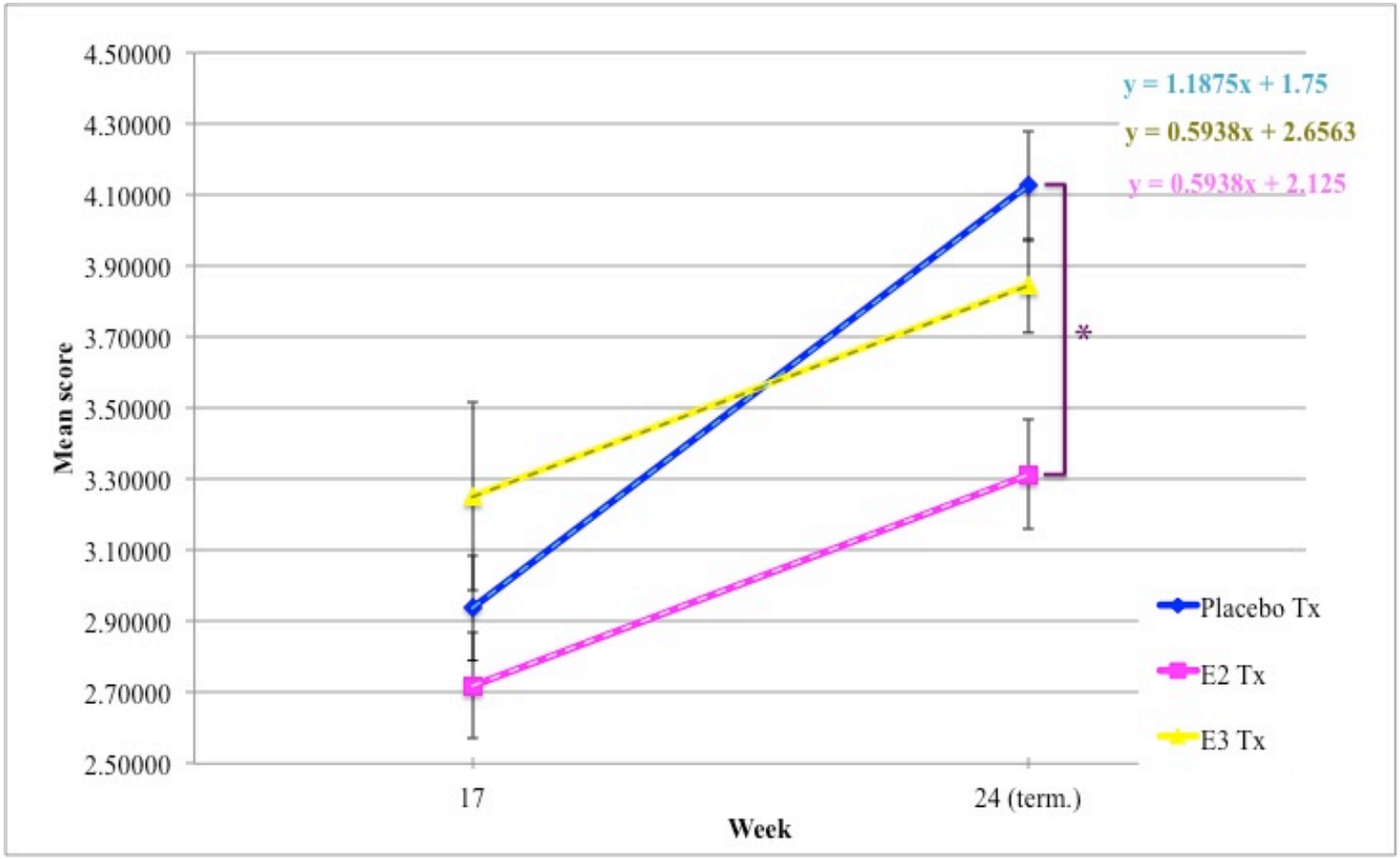

Figure 3.2 Mean clinical scores from weeks 17 and 24 show an increase in severity over the observation period.
No significant difference was found among groups during week 17 ($p>0.05$). Group scores were significantly different at termination (week 24) ($p<0.05$). Though E_2-treatment and E_3-treatments both had the same slope, E_2-treatment group scores remained lower than both E_3 and Placebo-treated group scores.

3.2 Hormone Replacement Treatment Post-ovariectomy Causes Uteri to Increase in Size and Weight

The mean uterine weights for both the uninfected and infected groups and hormone treatment subgroups are presented in Table 3.3. The uteri were collected and weighed after sacrificing the mice on week 24 of the experiment. The uteri were used to assess the effect of the hormones on the mice post-ovariectomy. Figure 3.3 presents the mean weight of the uteri graphically. A Two-way Analysis of Variance (ANOVA) was done to evaluate the difference between both uninfected and infected mice and their respective hormone treatment subgroups. There was a very significant difference in uterine weights among groups ($F_{(5,43)}$: 68.098, $p<0.05$) that was influenced by hormone treatment ($F_{(2,43)}$: 166.696, $p<0.05$) but not infection with virus ($F_{(1,43)}$: 0.026, $p>0.05$). There was no interaction between virus and hormone ($F_{(2,43)}$: 1.186, $p>0.05$). Further analysis, using Least Squares Difference (LSD) *post hoc* test showed no significant difference in uterine weights between E_2 and E_3-treated mice in either group ($p>0.05$), but a significant difference between these groups and placebo-treated mice ($p<0.05$) in both infected and uninfected mice.

Table 3.3 Mean uterine weights in grams.
Mean uterine weights for each group are presented along with the standard error. The top row represents uninfected groups and the bottom row represents infected groups

	E_2+PBS n=7	E_3+PBS n=7	Placebo+PBS n=8
Avg	0.14614	0.14943	0.04288
SEM	0.00896	0.00803	0.00505
	E_2+Virus n=8	E_3+Virus n=8	Placebo+Virus n=6
Avg	0.15863	0.14250	0.03943
SEM	0.00821	0.00389	0.00290

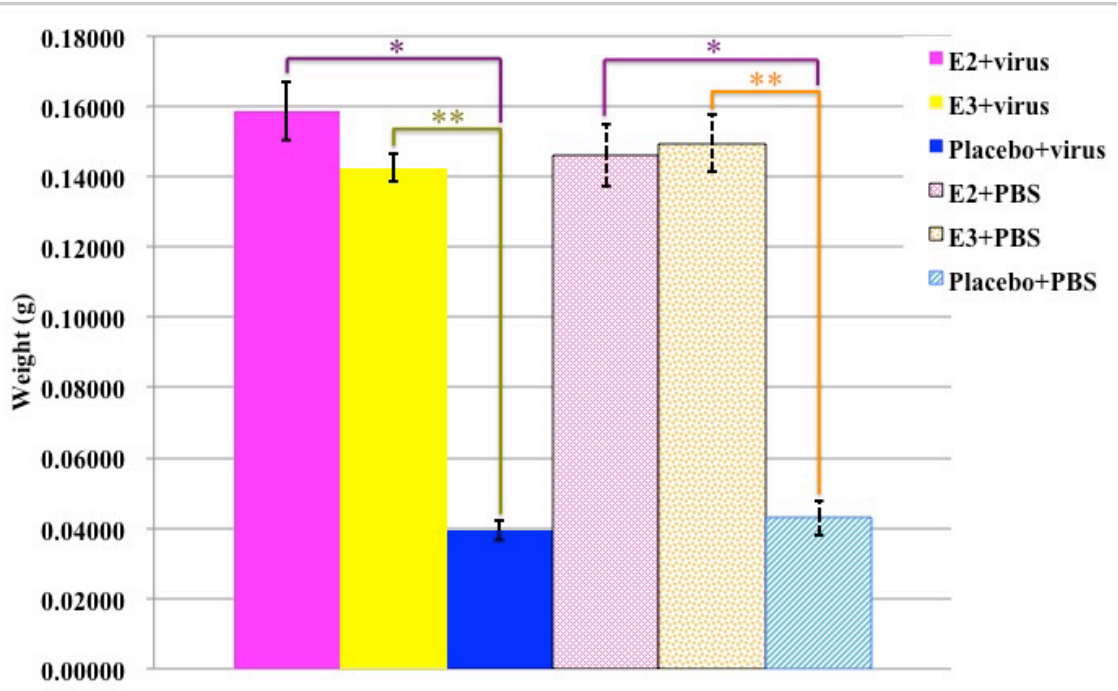

Figure 3.3 Graphical representation of the mean uterine weights obtained at termination. There was a significant difference among groups ($p<0.05$) with a main effect of hormone treatment ($p<0.05$). There was a significant difference between E_2 and placebo (*) as well as between E_3 and placebo groups in mean uterine weight (**) in both infected and uninfected groups. No significant difference ($p>0.05$) was found between E_2 and E_3-treated groups in either infected or uninfected groups. Data shown as Mean ± SEM. *$p<0.05$, **$p<0.05$

3.3 Infection with Theiler's Virus Has No Effect on Spleen Weights

The spleens were collected and weighed after sacrificing the mice on week 24. Their weights were used to assess immune activation. Table 3.4 presents the mean weights and standard errors for the uninfected and infected groups and their hormone treatment subgroups, respectively. The three infected groups seemed to have smaller spleens than the uninfected groups, however, this did not reach significance. Figure 3.4 presents the mean weight of the spleens graphically. A Two-way Analysis of Variance (ANOVA) was done to evaluate the difference between both uninfected and infected mice and their respective hormone treatment subgroups. There was no significant difference in spleen weights among groups ($F_{(5,43)}$: 1.599, $p>0.05$). Infection with virus had an effect on spleen weights ($F_{(1,43)}$: 7.912, $p<0.05$); however, hormone treatment

had no effect ($F_{(2,43)}$: 0.004, p>0.05). There was no interaction between virus and hormone ($F_{(2,43)}$: 0.012, p>0.05).

Table 3.4 Mean splenic weights in grams.
Mean splenic weights for each group are presented along with the standard error. The top row represents uninfected groups and the bottom row represents infected groups

	E_2+PBS n=7	E_3+PBS n=7	Placebo+PBS n=8
Avg	0.13271	0.13200	0.13175
SEM	0.00984	0.00581	0.00467
	E_2+Virus n=8	E_3+Virus n=8	Placebo+Virus n=6
Avg	0.11613	0.11463	0.11500
SEM	0.00873	0.00729	0.00572

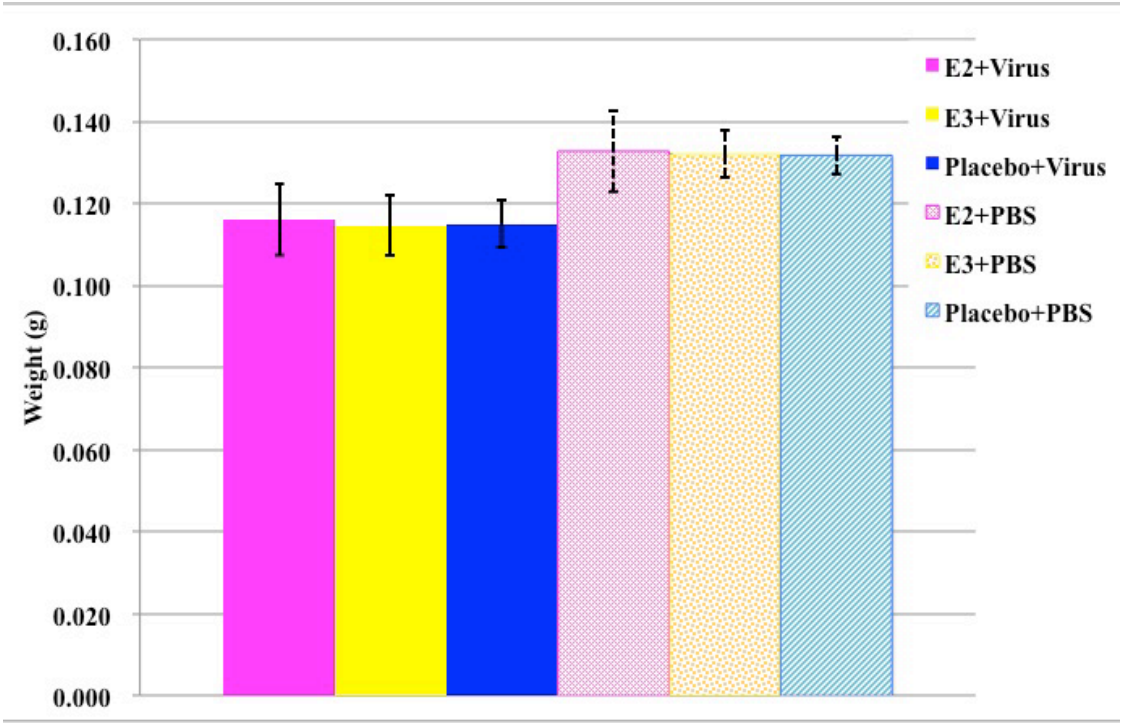

Figure 3.4 Graphical representation of mean splenic weights obtained at termination.
There was no significant difference among groups (p>0.05) despite having a main effect of infection with virus (p<0.05). Data shown as Mean ± SEM.

3.4 Treatment with E_2 and E_3 Diminishes the Percent Inflammation in the Spinal Cord Sections Compared to Placebo Treatment

As previously mentioned, inflammatory lesions of the spinal cord characterize the Theiler's Murine Encephalomyelitis Virus (TMEV) model. Area measurements were used to determine percent inflammation in the different spinal cord segments. We measured perivascular cuffing (accumulation of leukocytes around blood vessels) at 40x magnification. In addition, a note was made of areas with *status spongiosus*, which represent areas where demyelination may be inferred using H&E.

The TMEV model's inflammatory lesions are commonly found in cervical and thoracic spinal cord sections. Figure 3.5 A-D shows a representative sampling from each group using cervical spinal cord sections. The sections selected as representative for each treatment group had the mean scores of inflammation of that particular experimental group. All sections were taken at 40x magnification and were edited using SketchbookExpress (Autodesk) to remove excess structures (bone, muscle, etc). Panel A depicts an uninfected mouse, panel B depicts a placebo-treated infected mouse, panel C depicts an E_2-treated infected mouse, and Panel D shows an E_3-treated infected mouse. Within each panel, the red circles indicate perivascular cuffing and the red arrows represent *status spongiosus*, or the beginnings of demyelination. Similarly, Figure 3.6 A-D shows a representative sampling in a similar manner but using thoracic spinal cord sections.

Total cord area, gray matter area, and area of inflammation (sum of areas, including cuffing and parenchymal) were obtained using ImageJ (NIH). The white matter area was calculated and these data were used to obtain a percent white matter inflammation. The data was collected per mouse and later compiled leaving only white matter area and area of inflammation. These numbers were used to obtain a global percent inflammation per mouse and the averages and standard errors are presented in Table 3.5. This was the data used for statistical analysis. One-Way Analysis of Variance (ANOVA) with a Least Squares Difference (LSD) *post hoc* test was used to analyze the differences between groups. There was a significant difference among groups in

inflammation ($F_{(2,21)}$: 8.770, $p<0.05$). The LSD *post hoc* test revealed there was also significant difference between E_2 and placebo ($p<0.05$), E_3 and placebo ($p<0.05$), and between E_2 and E_3-treated groups ($p<0.05$) indicating an overall effect of treatment with E_2 having the greatest effect. Figure 3.7 presents the compiled data graphically as Mean ± SEM.

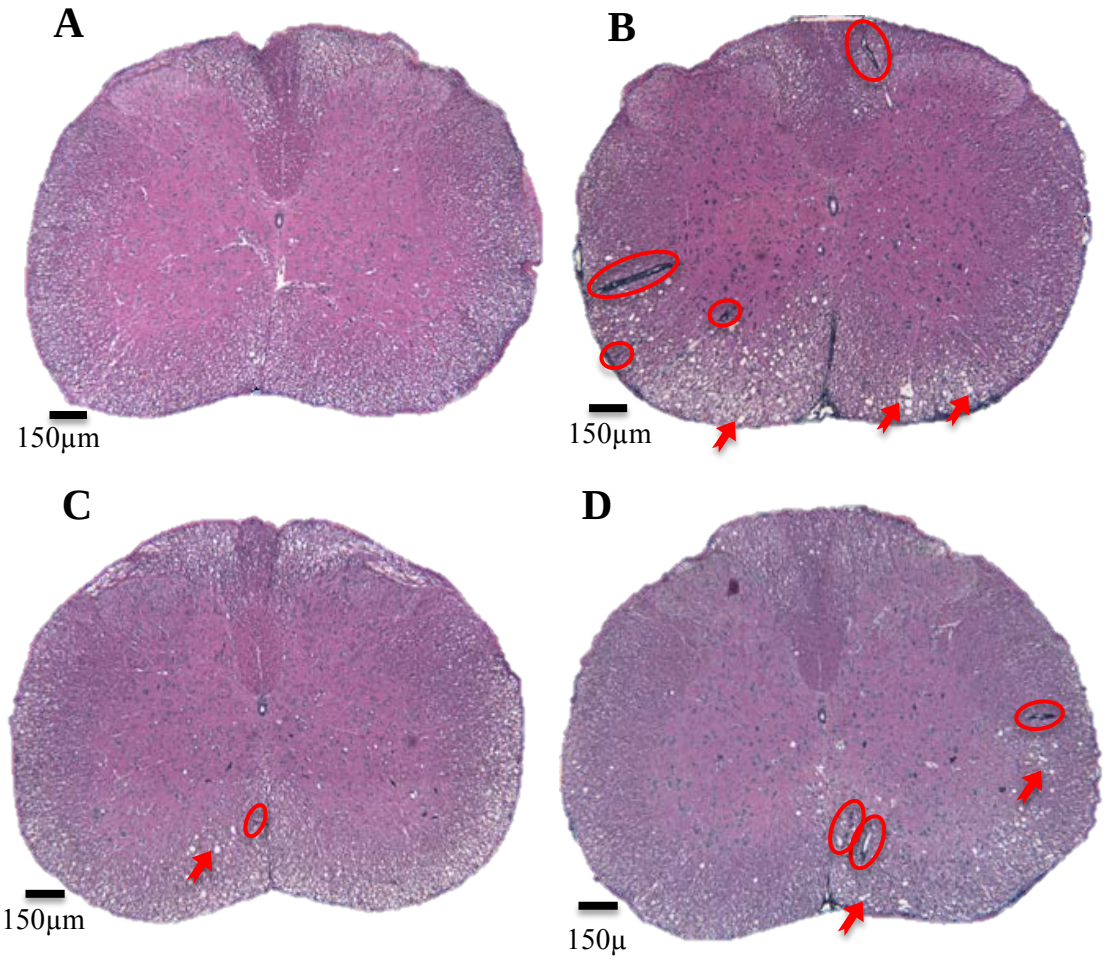

Figure 3.5 H&E-stained cervical spinal cord sections from control and three different treatment groups.
Panel A depicts a placebo-treated uninfected mouse. Panel B represents a placebo-treated infected mouse. Panel C represents an E_2-treated infected mouse. Panel D represents an E_3-treated infected mouse. The red circles depict areas of perivascular infiltration and the red arrows represent areas of parenchymal inflammatory infiltration and *status spongiosus*. All images captured at 40x magnification

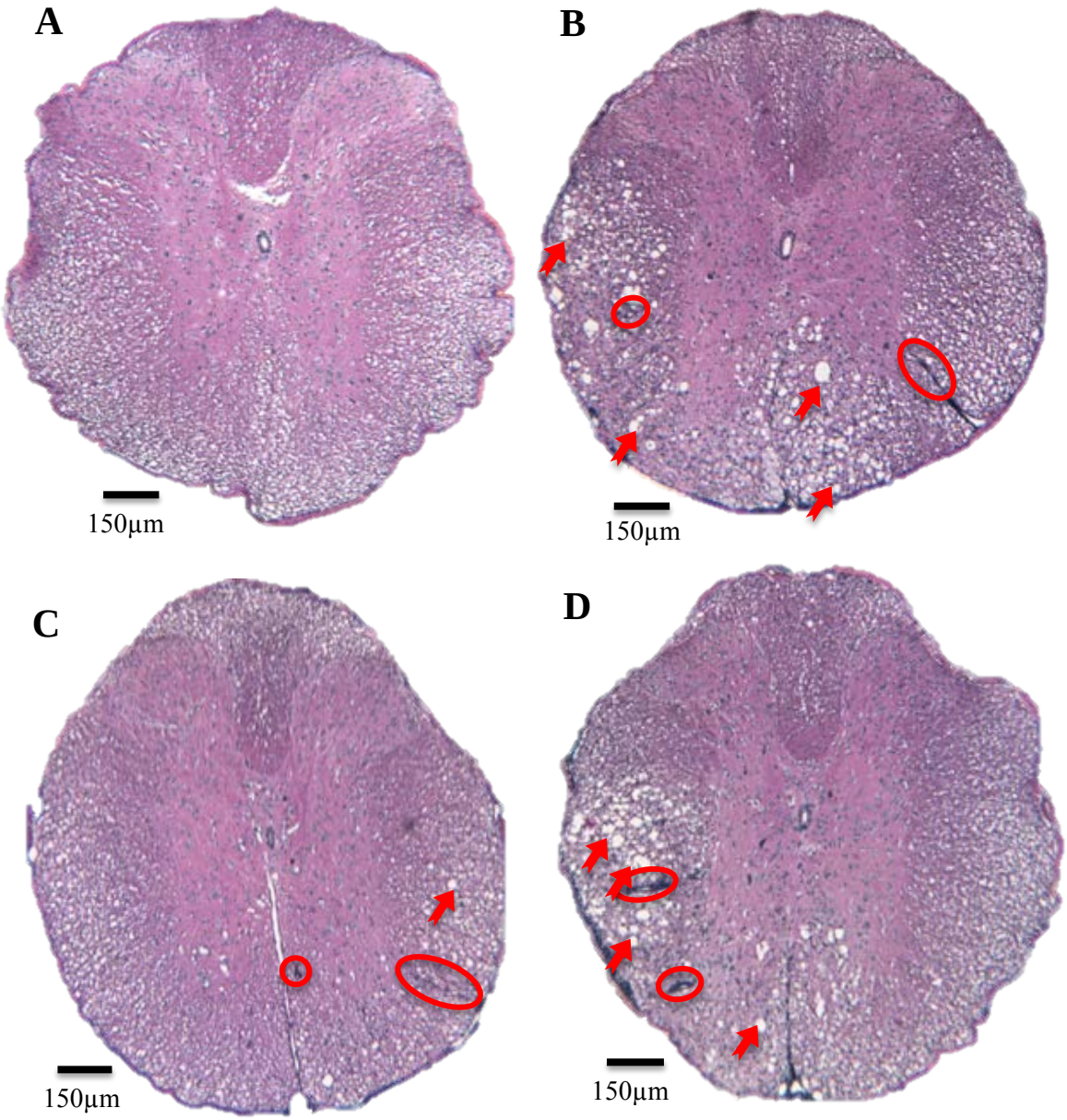

Figure 3.6 H&E-stained thoracic spinal cord sections from control and three different treatment groups.
Panel A depicts a placebo-treated uninfected mouse. Panel B represents a placebo-treated infected mouse. Panel C represents an E_2-treated infected mouse. Panel D represents an E_3-treated infected mouse. The red circles depict areas of perivascular infiltration and the red arrows represent areas of parenchymal inflammatory infiltration and *status spongiosus*. All images captured at 40x magnification

Table 3.5 Mean percent white matter inflammation.
The mean percent inflammation and standard errors are presented for each treatment group

	Placebo Tx n=6	E_3 Tx n=8	E_2 Tx n=8
Mean	0.76068	0.49727	0.25470
SEM	0.10324	0.09385	0.05026

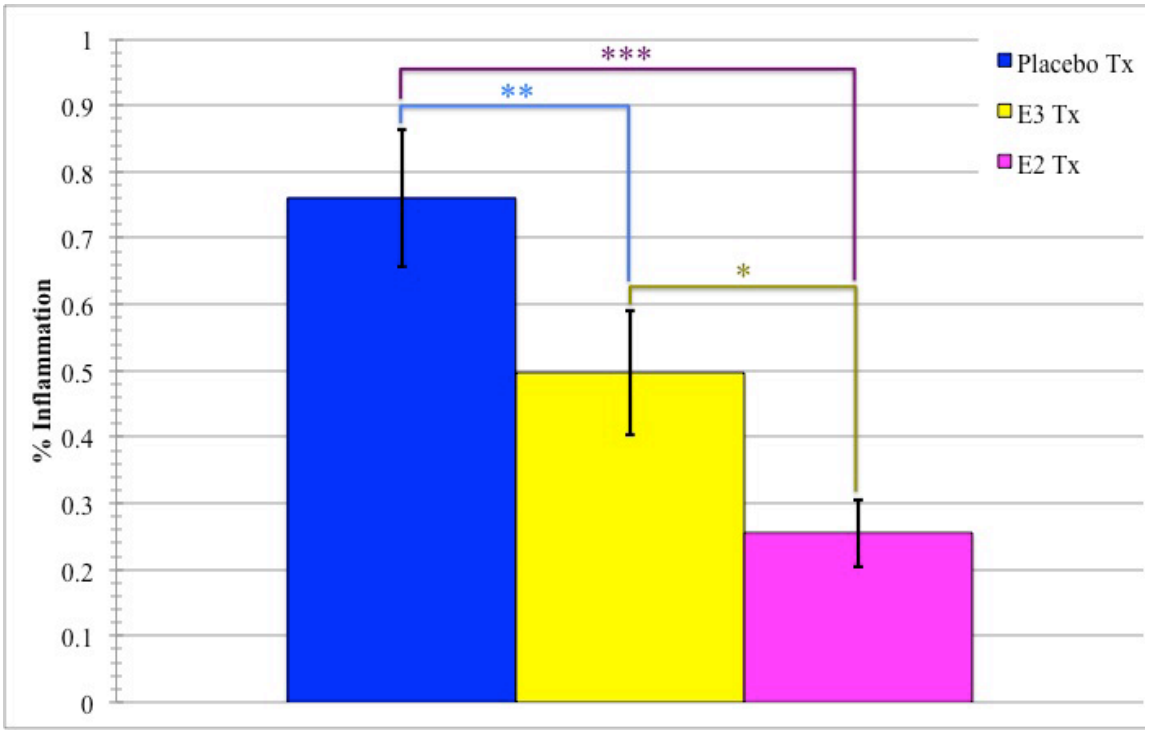

Figure 3.7 Graphical representation for the mean white matter inflammation per treatment group.
There is a significant difference among all three groups ($p<0.05$). *Post hoc* tests revealed a significant difference between E_2 and E_3-treated groups (*), E_3 and placebo groups (**), and between E_2 and placebo groups (***). Data presented as Mean ± SEM. *$p<0.05$, **$p<0.05$, ***$p<0.05$

3.5 Treatment with E_2 Reduces Demyelination in the Spinal Cord When Compared to Placebo

The Weil's stain for myelin was used to detect demyelination. We identified and outlined areas of demyelination at 40x magnification.

Similar to the location of inflammatory lesions, demyelinating lesions in TMEV are also found on primarily in cervical and thoracic spinal cord sections. Figure 3.8 A-D show a representative sampling from each group using cervical spinal cord sections. The sections selected as representative for each treatment group had the mean scores of demyelination of that particular experimental group. All sections were taken at 40x magnification and were edited using SketchbookExpress (Autodesk) to remove excess structures (bone, muscle, etc.). Panel A in Figure 3.8 depicts an uninfected mouse, panel B depicts a placebo-treated infected mouse, panel C depicts a E_2-treated infected mouse, and Panel D shows an E_3-treated infected mouse. Within each panel, the red arrows indicate areas of demyelination. Similarly, Figure 3.9 A-D shows a representative sampling using thoracic spinal cord sections.

Once again, three measurements were obtained from each section: Total cord area, gray matter area, and area of demyelination (sum of areas) if applicable. The white matter area affected was obtained from calculations and used to obtain a percent white matter demyelination. The white matter area was calculated and these data were used to obtain a percent white matter demyelination. The data was collected per mouse and later compiled leaving only white matter area and area of demyelination. These numbers were used to obtain a global percent demyelination per mouse and the averages and standard errors are presented in Table 3.6. This was the data used for statistical analysis. One-Way Analysis of Variance (ANOVA) with a Least Squares Difference (LSD) *post hoc* test was used to analyze the differences between groups. There was a significant difference among groups in inflammation ($F_{(2,21)}$: 4.732, $p<0.05$). The LSD *post hoc* test revealed there was also significant difference between E_2 and placebo ($p<0.05$). No significant difference was found between E_3 and placebo ($p>0.05$), or between E_2 and

E_3-treated groups (p>0.05). Figure 3.10 presents the compiled data graphically as Mean ± SEM.

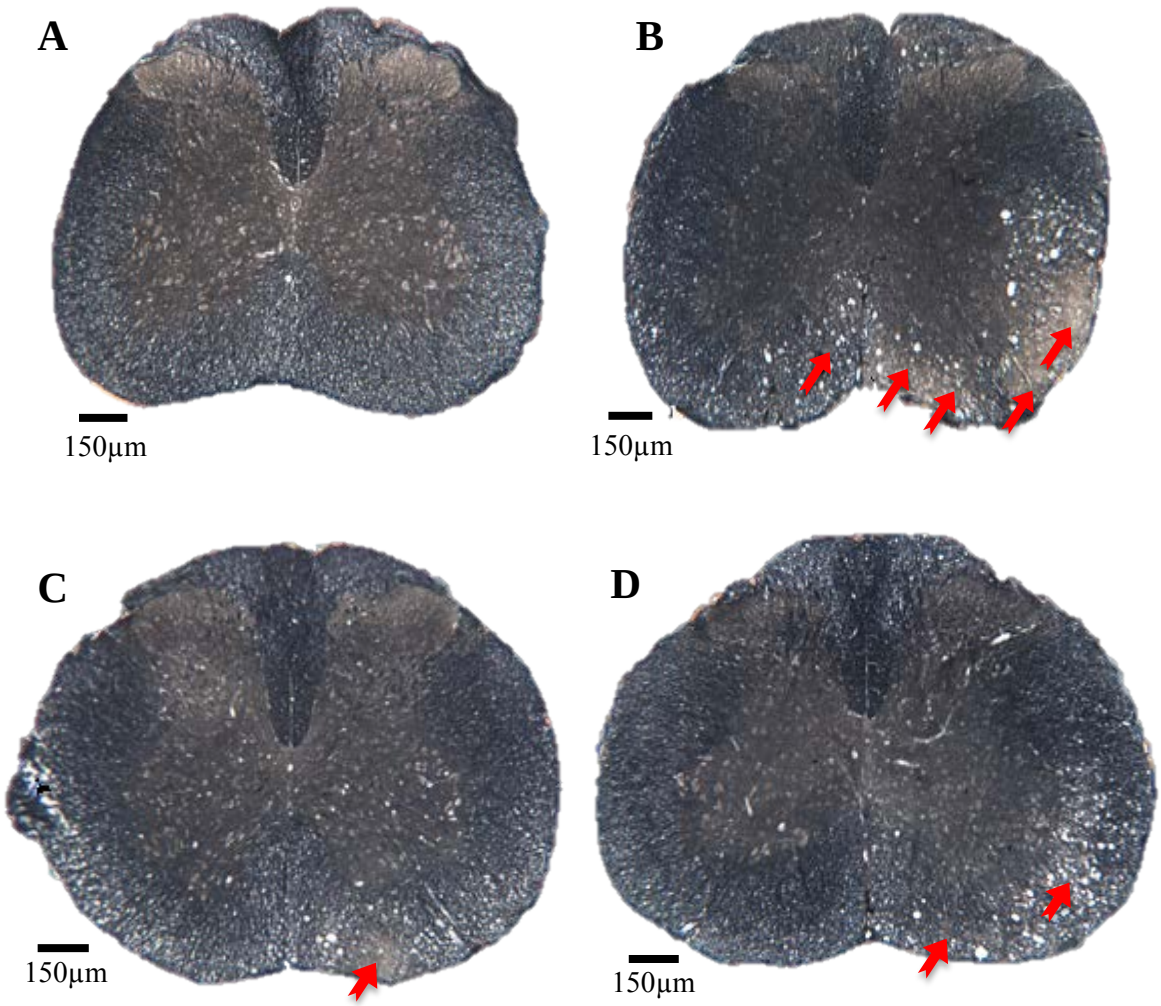

Figure 3.8 Weil's-stained cervical spinal cord sections from control and three different treatment groups.
Panel A depicts a placebo-treated uninfected mouse. Panel B represents a placebo-treated infected mouse. Panel C represents an E_2-treated infected mouse. Panel D represents an E_3-treated infected mouse. The red arrows show areas of demyelination. Panel D is at the early stages of demyelination and the arrows point to primarily *status spongiosus* with the left arrow pointing at a small area of demyelination. All images captured at 40x magnification

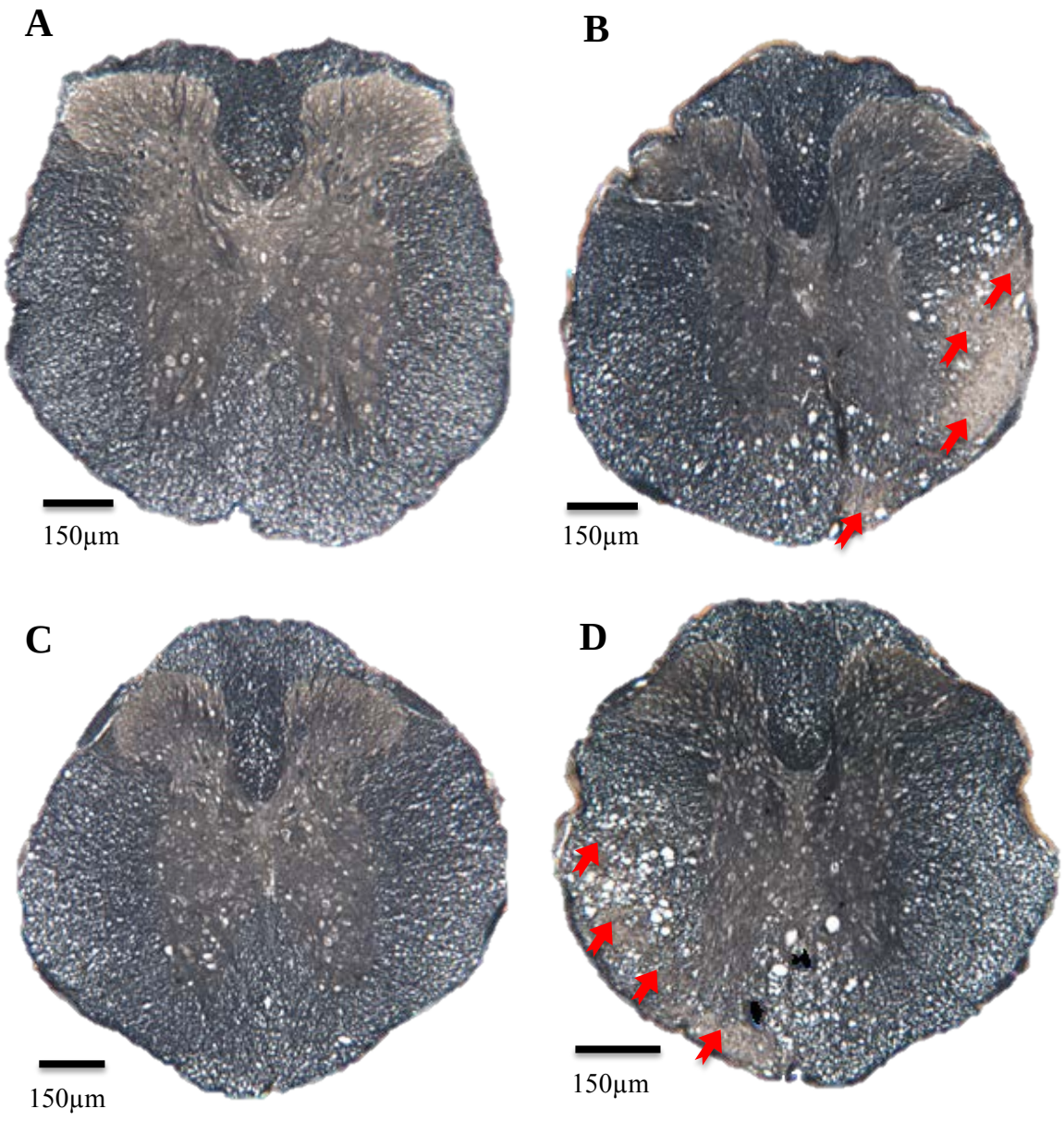

Figure 3.9 Weil's-stained thoracic spinal cord sections from control and three different treatment groups.
Panel A depicts a placebo-treated uninfected mouse. Panel B represents a placebo-treated infected mouse. Panel C represents an E_2-treated infected mouse. Panel D represents an E_3-treated infected mouse. The red arrows show areas of demyelination. Panel C shows no apparent signs of demyelination. All images captured at 40x magnification

Table 3.6 Mean percent white matter demyelination.
The mean percent white matter demyelination and standard errors are presented for each treatment group

	Placebo Tx n=6	E_3 Tx n=8	E_2 Tx n=8
Mean	13.35095	8.07803	4.54065
SEM	2.02817	2.27615	1.47107

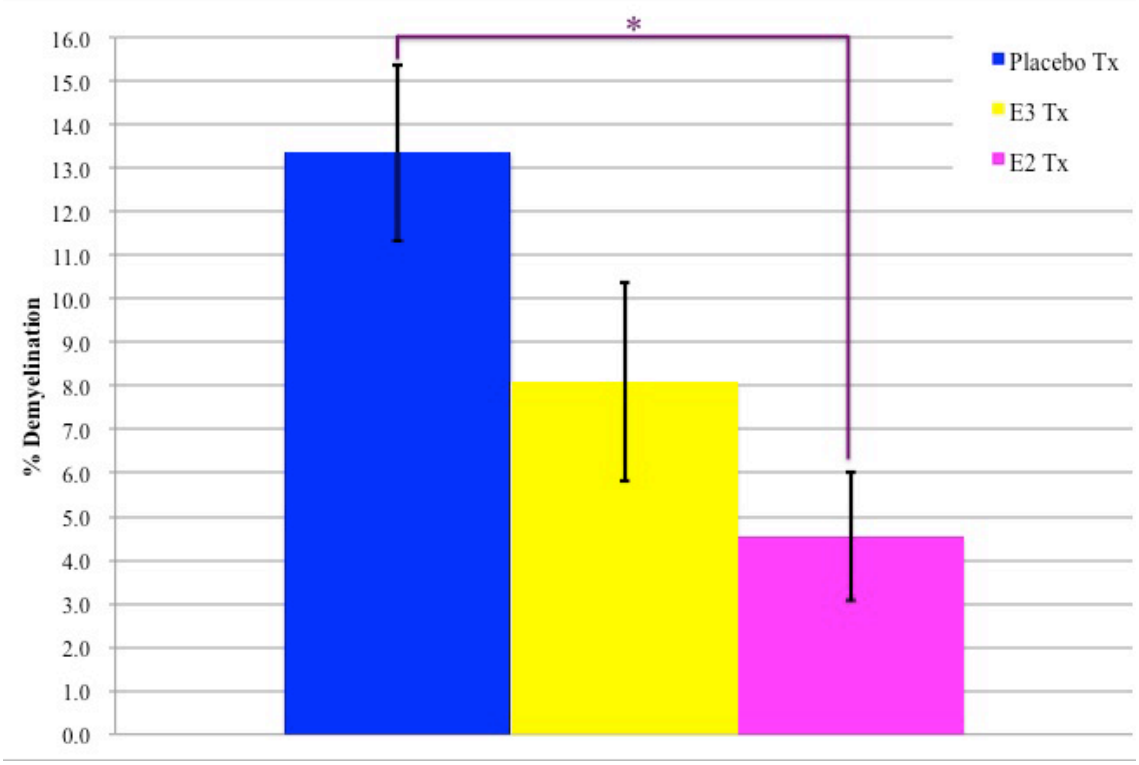

Figure 3.10 Graphical representation of the mean percent white matter demyelination per group.
There is a significant difference in percent white matter demyelination among all three groups ($p<0.05$). *Post hoc* tests revealed no significant difference between E_2 and E_3-treated groups ($p>0.05$), or E_3 and placebo groups ($p>0.05$). However, there was a significant difference between E_2 and placebo groups (*). Data presented as Mean ± SEM. *$p<0.05$

3.5.1 Serial Section Comparison between H&E and Weil's-stained Spinal Cord Sections Allow Visual Co-localization of Inflammatory and Demyelinating Lesions

H&E sections from representative mice were chosen as described previously and matched to the Weil's stain serial sections to visually correlate inflammatory lesion location to demyelinating lesion location. All sections were captured at 40x magnification and were edited using SketchbookExpress (Autodesk) to remove excess structures (bone, muscle, etc.). Figure 3.11 A-D depict serial cervical sections. Row A represents cervical sections from control-uninfected mice from H&E and Weil's stains, respectively. Row B represents sections from placebo-treated mice, row C represents E_2-treated infected mice, and row D represents E_3-treated infected mice in the same manner as described above. Figure 3.12 A-D depict serial thoracic sections. Row A represents thoracic sections from control uninfected mice from the infection and demyelination studies, respectively. Row B represents sections from placebo-treated mice, row C represents E_2-treated infected mice, and row D represents E_3-treated infected mice in the same manner as described above.

All the serial sections that show inflammation, also have signs of demyelination that can be co-localized to areas near perivascular cuffing and areas that show *status spongiosus* in H&E-stained sections.

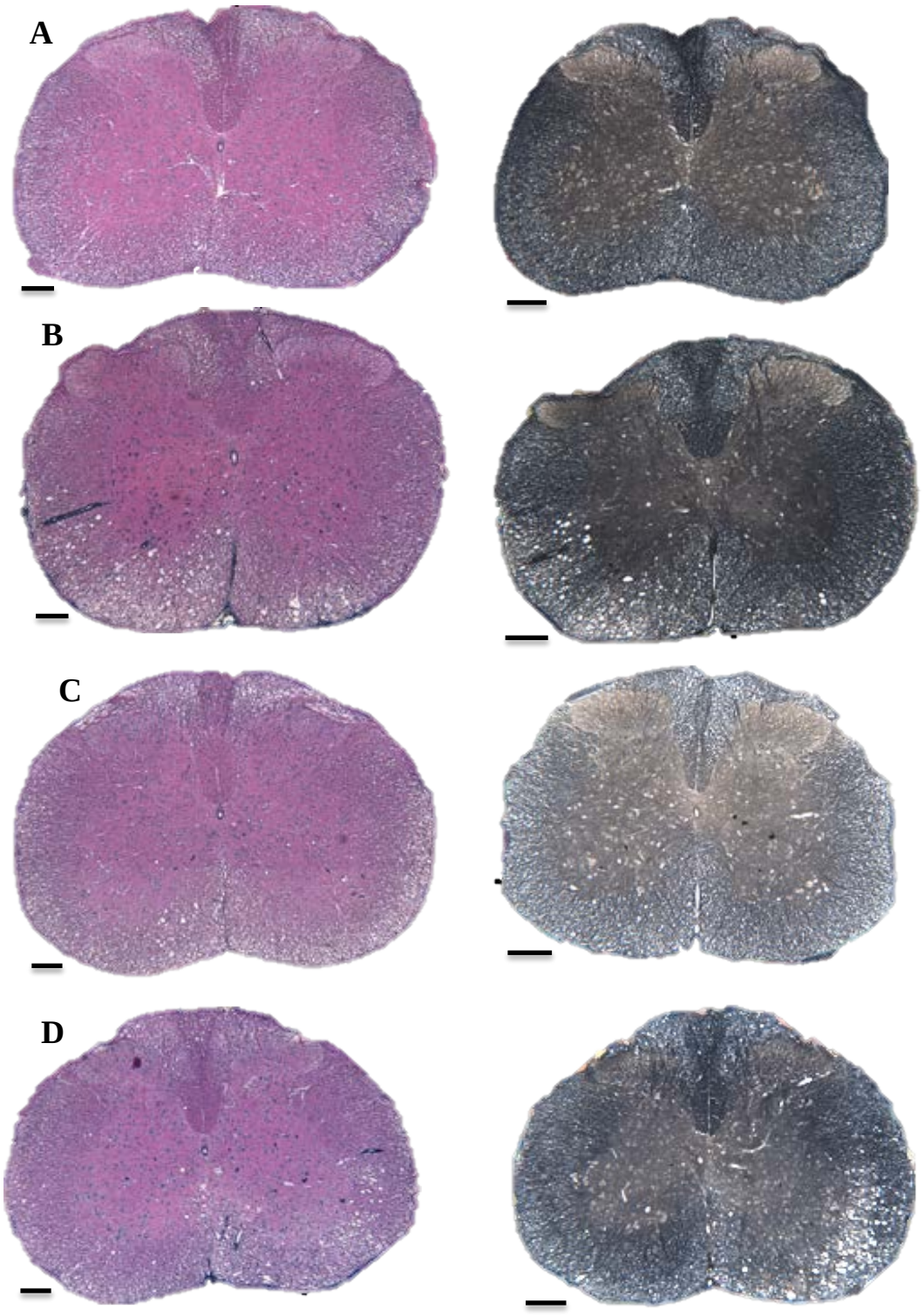

Figure 3.11 Cervical spinal cord serial section comparisons between H&E (inflammation) and Weil's (demyelination) stains.
Row A represents control-uninfected mice, B represents placebo-treated infected mice, C represents E_2-treated infected mice and D represents E_3-treated infected mice. Bar = 150µm. 40x magnification

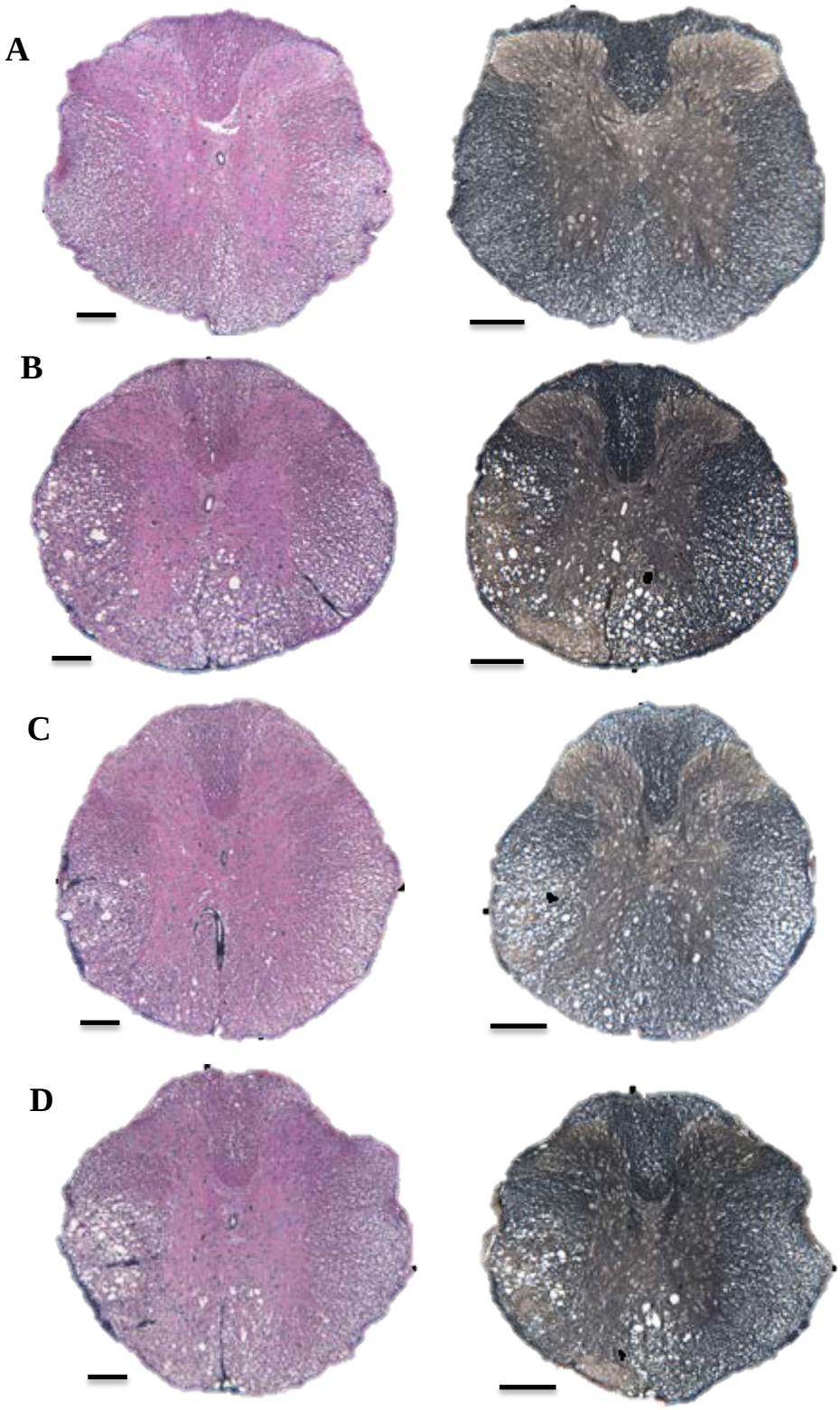

Figure 3.12 Thoracic spinal cord serial sections between H&E (inflammation) and Weil's (demyelination) stains.
Row A represents control-uninfected mice, B represents placebo-treated infected mice, C represents E_2-treated infected mice and D represents E_3-treated infected mice. Bar = 150µm. 40x magnification

3.6 Radio-immuno Assay Measurements of Theiler's Virus Antibody (Ab) Levels Show Differences between Infected and Uninfected Groups and That Both E_2 and E_3-Treatments Differ from Placebo in the Infected Groups

Radio-Immuno (RIAs) for Theiler's virus antibody (GD-VII) were conducted on the sera collected from the mice at termination. The data was compiled and averaged by group to create Tables 3.7 and 3.8 and graphed as counts per minute (CPM) versus dilution as shown in Figure 3.13. Figure 3.14 shows the graphed CPM vs. dilution values for the infected groups only. By the 1/160 dilution, there are no detectable differences among control or infected groups.

A Two-way Analysis of Variance (ANOVA) was done to evaluate the difference between both uninfected and infected mice and their respective hormone treatment subgroups at the 1/40 dilution, as this dilution is a good representative choice for the range of dilutions up to 1/160. There was a significant difference in Theiler's Virus antibody (Ab) levels among groups ($F_{(5,43)}$: 6.447, p<0.05). Infection with virus had a significant effect on Ab levels ($F_{(1,43)}$: 15.124, p<0.05) as did hormone treatment ($F_{(2,43)}$: 7.841, p<0.05). There was no interaction between virus and hormone ($F_{(2,43)}$: 2.780, p>0.05) at the 1/40 dilution. *Post hoc* Least Squares Difference (LSD) analysis revealed that there was a significant difference between placebo and E_3 (p<0.05) and between placebo and E_2 (p<0.05) in the 1/40 dilution. No significant difference was found between E_3 and E_2 (p>0.05).

A comparison of only the infected groups using 1-way ANOVA revealed similar significant differences among the three groups in the 1/40 dilution ($F_{(2,21)}$: 5.579, p<0.05)). *Post hoc* Least Squares Difference (LSD) analysis revealed that there was a significant difference between placebo and E_3 (p<0.05) and between placebo and E_2 (p<0.05) at the 1/40 dilution. No significant difference was found between E_3 and E_2 (p>0.05).

Table 3.7 Average RIA counts per minute for treated, uninfected groups.
The mean counts per minute for serial dilutions from 1/20 to 1/160 are presented in this table for each uninfected and treated mouse group. The 1/40 dilution was used for statistical analysis

Control (n=8)				
Dilution	1/20	1/40	1/80	1/160
Average	610.500	390.875	266.250	202.125
SEM	200.219	114.143	63.818	59.379
E_3 Control (n=7)				
Dilution	1/20	1/40	1/80	1/160
Average	307.857	194.857	147.429	115.143
SEM	77.346	40.130	17.389	4.758
E_2 Control (n=7)				
Dilution	1/20	1/40	1/80	1/160
Average	401.143	182.857	164.857	142.857
SEM	178.105	15.251	14.287	13.869

Table 3.8 Average RIA counts-per-minute for treated, infected groups.
The mean counts per minute for serial dilutions from 1/20 to 1/160 are presented in this table for each infected and treated mouse group. The 1/40 dilution was used for statistical analysis

Placebo Tx (n=6)				
Dilution	1/20	1/40	1/80	1/160
Average	1,797.667	1,142.000	761.833	477.500
SEM	446.942	328.822	210.086	112.335
E_3-Tx (n=8)				
Dilution	1/20	1/40	1/80	1/160
Average	475.500	315.500	262.875	222.875
SEM	86.689	45.293	33.625	16.576
E_2-Tx (n=8)				
Dilution	1/20	1/40	1/80	1/160
Average	976.250	577.375	399.750	299.250
SEM	217.872	112.100	67.546	60.535

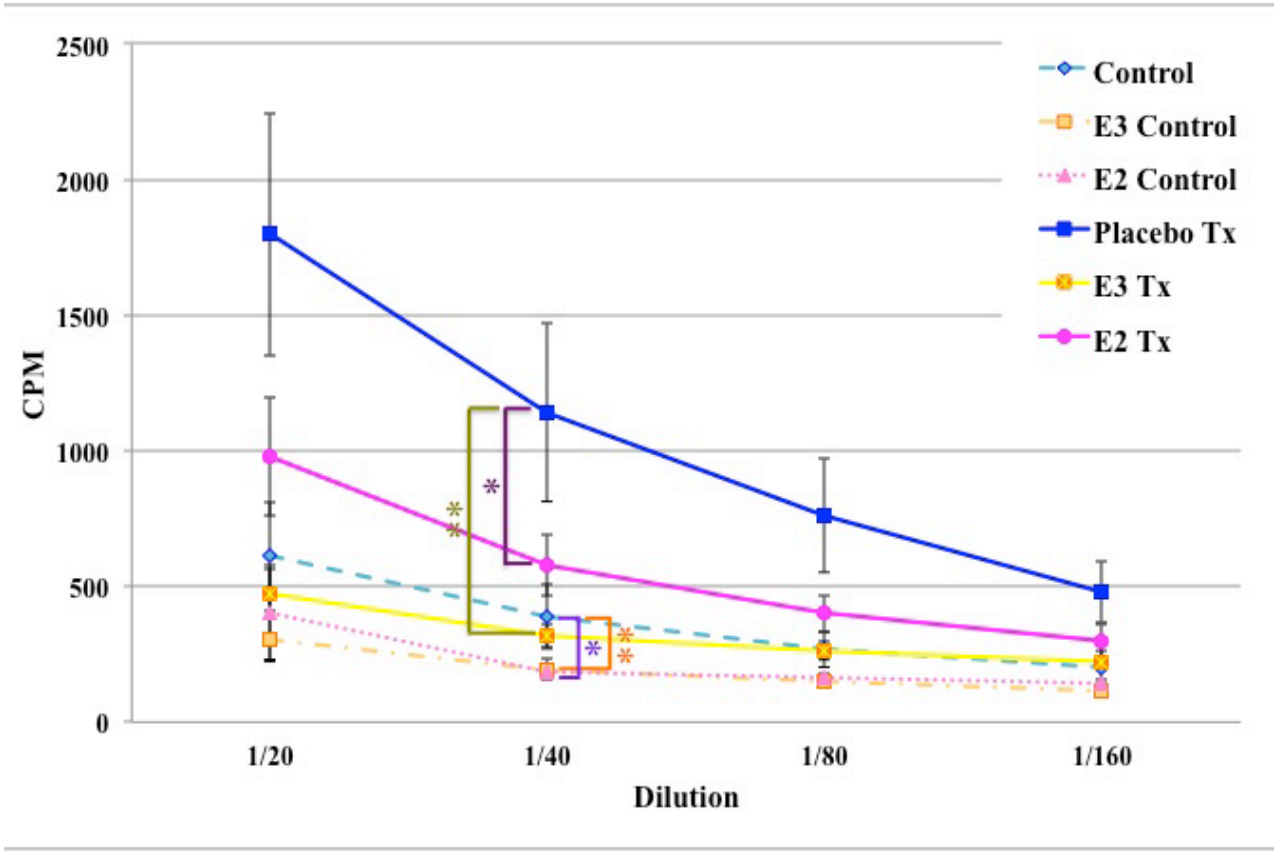

Figure 3.13 Radio-immuno assay analysis for TMEV antibody levels in the sera of uninfected and infected mice.
Data for the 1/40 dilution was chosen as a representative sample for the assay. Dashed lines represent control-uninfected groups and the solid lines represent treated-infected groups. There was a significant difference among groups in Ab levels to TMEV ($p<0.05$) with a main effect of virus infection ($p<0.05$) and hormone treatment ($p<0.05$). There was no interaction between virus and hormone ($p>0.05$). There was a significant difference between E_2 and placebo (*) as well as between E_3 and placebo groups for TMEV Ab levels (**) in both infected and uninfected groups. No significant difference ($p>0.05$) was found between E_2 and E_3-treated groups in either infected or uninfected groups. Data shown as Mean ± SEM. *$p<0.05$, **$p<0.05$

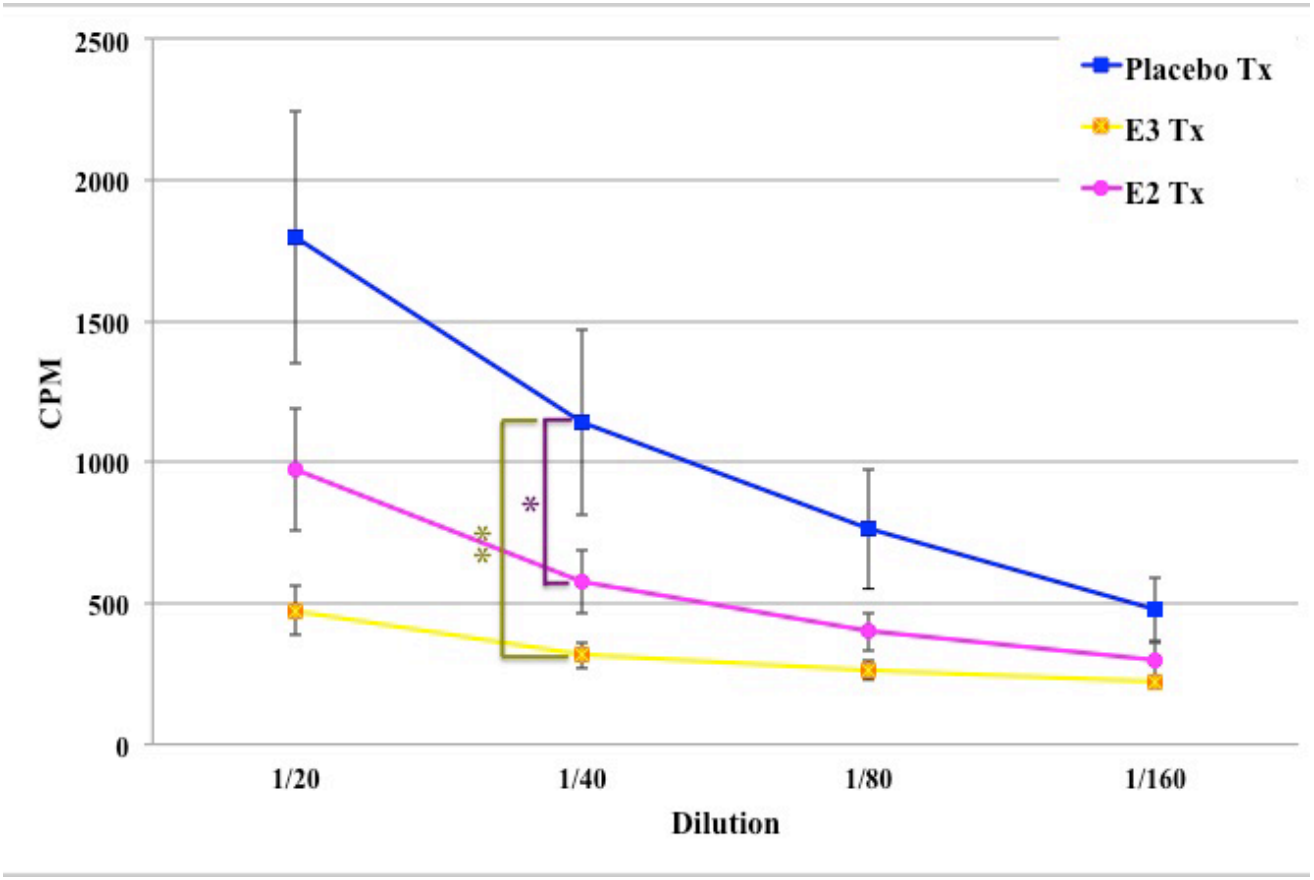

Figure 3.14 Radio-immuno assay analysis for TMEV antibody levels in the sera of infected mice
This graph presents the data for the 1/40 dilution of TMEV infected groups only. There is a significant difference ($p<0.05$) among all three groups in Ab levels. No significant difference was found between E_3 and E_2 ($p>0.05$). Placebo treated mice differ significantly from both E_2-treated (*) and E_3-treated mice (**). Data is presented as Mean±SEM. *$p<0.05$, **$p<0.05$

4. DISCUSSION

This project assessed the effect of hormone-replacement therapy on the chronic phase of Theiler's Murine Encephalomyelitis Virus (TMEV) infection. The data analysis focused on observations from week 15 post-infection (pi), which corresponds to week 17 of the experiment. Chronic demyelination in the Theiler's infection model is considered to begin 2-5 months pi and remain for the life of the mouse causing progressive disease similar to progressive human multiple sclerosis (Miller *et al*., 1995). For our treatments, we chose a 0.1mg pellet based on previous experiments performed by Bebo *et al.*, which indicated this dose, equivalent to diestrus levels of 17-β-estradiol (E_2) in mice (25-50pg/mL) was effective in significantly reducing EAE clinical scores compared to placebo (Bebo *et al*., 2001). Because estriol (E_3) is a hormone of pregnancy produced by the fetal-placental unit (Sicotte *et al*., 2002), we used information from Bebo *et al.* and from Palaszynski *et al.* to select a 5.0mg E_3 pellet, which would give pregnancy hormone level equivalents (2000-3000pg/mL), this level of E_3 in circulating blood reduced incidence of EAE compared to placebo (Bebo *et al*., 2001; Palaszynski *et al*., 2004). The levels of E_2 and E_3 chosen led to increases in uterine size. For both infected and uninfected groups, the weight of the uteri was significantly different than placebo-treated mice. Because the mice were ovariectomized, this measurement allowed us to determine the effectiveness of the hormone replacement. Our results indicate that the doses of E_2 and of E_3 we selected have a positive effect on inflammation. The spleen is an important secondary lymphoid organ, our results showed that the spleens in the infected groups on average weighed less than those of the uninfected groups; however, our results showed no significance in weight. This is consistent with findings by Mendez-Fernandez *et al.*, who showed the spleen was not necessary for TMEV-specific $CD8^+$ cell-activation and recruitment (Mendez-Fernandez *et al*., 2005).

The current study showed that E_2 has therapeutic effects on the Theiler's Virus-Induced Demyelination (TVID) model of multiple sclerosis. Our experiments demonstrated that treating young ovariectomized female mice with estradiol reduced clinical signs of disease as well as histological signs of inflammation and demyelination

in the spinal cord. These findings were consistent with our hypothesis. Treatment with E_3 also was effective in reducing signs of inflammation; however, it showed no difference from placebo-treated mice in improvement of clinical scores or demyelination. In the experimental autoimmune encephalitis (EAE) model, females that were ovariectomized but not treated did not show altered disease severity when compared to placebo-treated non-ovariectomized mice. This indicates that physiological levels of estrogens may not be enough to cause any effect on disease progression in this model once the disease has begun (Voskuhl and Palaszynski, 2001). Conflicting results were shown if treatment with physiologic levels of E_2 and E_3 were administer prior to the onset of EAE (Bebo *et al*., 2001). Ovariectomy may have been a factor for the lessened effect of E_3 in our experiment; however, EAE model is a pure autoimmune model that does not account for the effects of the virus present in TVID; rather it directs a $CD4^+$ response to myelin components (Miller *et al*., 1995). Nevertheless, E_3 has been shown to be protective in studies with human MS patients and in the non-ovariectomized EAE model of MS (Palaszynski *et al*., 2004; Sicotte *et al*., 2002; Spence and Voskuhl, 2012). It is difficult to assess the reason behind the inability of E_3 treatment to diminish demyelination. Perhaps the length of treatment was not sufficient to allow the hormone to have an effect.

The discrepancy in our results could be explained by differences in the binding of estriol *versus* estradiol to estrogen receptors (ERs). Both estriol and estradiol can bind to estrogen receptors α and β (ERα and ERβ, respectively). However, estradiol has a higher affinity for ERα while estriol has a higher affinity for ERβ (Spence and Voskuhl, 2012). ERα has been implicated in EAE as having a potent anti-inflammatory response. Binding of E_2 to ERα inhibits the transport of the pro-inflammatory transcription factor NF-κB into the nucleus via interaction with PI3K, most notably in microglia, the resident macrophages of the CNS (Spence *et al*., 2011; Vegeto *et al*., 2008). In ischemia, ERα-mediated suppression of these cells and other inflammatory cells seems to be responsible for neuroprotection in young female rats post-stroke (Selvamani and Sohrabji, 2010). *In vitro* experiments have shown that stimulation of ERα by E_2 or another agonist

suppresses transcription of NF-κB in astrocytes and TNF-α-mediated production of pro-inflammatory CCL2 (Giraud *et al*., 2010) and to modulate infiltration of peripheral lymphocytes into the CNS, whereas ERβ did not show any effect (Spence and Voskuhl, 2012). In addition, treatment with ERα ligand reduced spinal cord inflammation, whereas ERβ ligand treatment only showed protective effects in the long term, but no reduction in inflammation (Tiwari-Woodruff and Voskuhl, 2009). These observations help explain the relative abundance of inflammatory cells in the parenchyma of the spinal cord sections for E_3-treated mice *versus* E_2-treated mice in this project, as well as the decreased demyelination observed on the Weil's stained sections. One final observation is that E_2 increases the ability of astrocytes to resorb excess glutamate, thus preventing neuronal loss due to excitotoxicity and explaining the relative effectiveness of E_2 *versus* E_3 therapeutic effects on treated mice (Spence and Voskuhl, 2012).

The role of E_2 and astrocytes is more complex. Astrocytes are essential components of the blood-brain barrier (BBB), and they are important in cell-to-cell communication, not only in the CNS, but also with inflammatory cells (Kipp and Beyer, 2009). E_2 has been shown to prevent astrocytes from expressing MHC-II and to enhance the induction of T-cell apoptosis, via astrocytes by reduction of H^3-thymidine incorporation by the T-cells (Kipp and Beyer, 2009). Expression of ERα is necessary in astrocytes to prevent axonal loss, gliosis, and diminish or prevent lymphocyte and monocyte infiltration into the CNS (Spence *et al*., 2011). Estradiol is known to have positive effects in brain circulation and in young animal models, and reduce stroke severity (Cipolla *et al*., 2009; Selvamani and Sohrabji, 2010). The reduction in stroke severity is due to E_2's influence on the BBB, both endothelial cells and astrocytes. During stroke, edema causes damage to the parenchyma. Cipolla *et al.* found that ovariectomy in rats increases BBB permeability, but that treatment with E_2/E_3 combination therapy restores the integrity of the barrier almost to control level (Cipolla *et al*., 2009) The levels of E_2 found in this study are almost at the levels found at estrous in the rat ovarian cycle (Shaikh, 1971), making them a comparable measure to the dose of E_2 given in this study. A similar mechanism may also be taking place in our study:

with the maintenance of BBB integrity, less lymphocytes and macrophages would be able to migrate into the parenchyma, thus reducing inflammation. The Cipolla study did not clarify whether E_2 or E_3 had a more significant effect on BBB permeability.

The Theiler's virus model is effective in showing pathological signs consistent with human MS. This model is unique in its biphasic disease onset. Strains such as the Daniel's (DA) and BeAn strain set up an acute gray matter inflammation. Studies using Severe Combined Immunodeficient (SCID) mice, showed that the virus could infect neurons and glia early on (6h to 7d pi) in both SCID and immunocompetent mice establishing infection in the corpus callosum and in hippocampal pyramidal neurons (Njenga *et al*., 1997) leading to the development of pathological polioencephalomyelitis, though most mice remain asymptomatic (Sato *et al*., 2011). In addition, SCID mice had virus in neuronal cell bodies in the spinal cord after 7d pi compared to immunocompetent mice. This indicated that virus was cleared before 7d pi in immunocompetent mice. This study revealed that both cellular and humoral immune responses are clearing the virus from gray matter, with the humoral branch being less efficient and also that both $CD4^+$ and $CD8^+$ cells have similar functions in gray matter viral clearance (Njenga *et al*., 1997).

It is not entirely clear why the virus cannot be fully cleared from white matter. It has been shown that it can persist in, macrophages, oligodendrocytes, axons, or glia, and that the attempt to clear it may be the main cause of the demyelinating chronic pathology that follows acute infection (Njenga *et al*., 1997; Sato *et al*., 2011). Infection in the TMEV model seems to be modulated by T_H1 mechanisms and based on our results, inflammation in the spinal cord parenchyma corresponds to areas of demyelination. This confirms the previous observation. A possible mechanism for the observed pathogenesis of TMEV can be elucidated from observations done by previous groups and observations from this work. The virus is capable of causing damage to axons, and by consequence to myelin and oligodendrocytes or directly infect and kill oligodendrocytes (Sato *et al*., 2011).

It was determined that the L-protein in Theiler's virus can inhibit gene

transcription, interfere with translation by preventing the export of mRNA from the nucleus, and regulate apoptotic signals. Thus the L-protein can cause cell death without inflammation (Ghadge *et al*., 2011). This may explain why the polioencephalomyelitis symptoms are limited. E_2 treatment has also been show to inhibit Theiler's virus replication (Kipp and Beyer, 2009), which may help explain the reduction in pathological findings in this treatment group.

Theiler's virus is unique among non-enveloped viruses in that it can exit a cell without lysis whereas other non-enveloped viruses need to lyse the cell once their replication is complete (Roussarie *et al*., 2007). This ability may help explain how TMEV is able to move from neuron to oligodendrocytes without causing neuronal cell death in the majority of cases and setting up a persistent infection in these white matter cells. Roussaire ***et al.*** propose that TMEV uses conventional cell machinery to migrate from axon to myelin and the group mentioned a hypothesis proposed by Gatzinski ***et al.*** which states axons may use myelin to remove unwanted materials, in this case virions (Roussarie *et al*., 2007). Because of the number of internodes and axons one oligodendrocyte can myelinate, its death can cause extensive demyelination. However, in the event of axonal damage, demyelination can also occur. Damage in the EAE model is accepted to come from "bystander" $CD4^+$-mediated injury to CNS tissue when these cells respond to myelin antigen, principally myelin proteolipid protein (PLP) (Sato *et al*., 2011) and myelin basic protein (MBP) is also involved in disease pathogenesis in EAE (Dal Canto *et al*., 2000). The PLP epitope used to induce EAE (PLP 139-152) seems to be involved in TMEV autoimmunity and as the disease progresses this epitope "spreads" to include other regions of the protein and other similar proteins such as Myelin Oligodendrocyte Glycoprotein (MOG) (Dal Canto *et al*., 2000).

Organotypic spinal cord cultures from SJL/J mice were prepared and treated with lymphocytes from TMEV-infected mice. They were then stimulated with MBP or PLP. Under MBP stimulation, the axons appeared normal and their numbers did not differ from naïve or sham-infected mice cultures; however, under PLP stimulation, the majority of the axons were heavily demyelinated (Dal Canto *et al*., 2000). These results

indicate that TMEV mechanisms of action may be different from the EAE model, where anti-MBP lymphocytes can cause culture demyelination and transfer disease to naïve mice (Dal Canto *et al*., 2000). EAE could be protected by anti-PLP Ab when whole myelin was used to prime the mice while anti-MBP Ab had no effect (Dal Canto *et al*., 2000). The TMEV model exhibited similar properties due to the liberation of myelin fragments early in the disease (Dal Canto *et al*., 2000). In addition $CD8^+$ T-cells expressing MHC-I infiltrate the CNS to clear the virus, but in doing so cause damage to myelin by recognizing self-epitopes (Sato *et al*., 2011; Tsunoda *et al*., 2005). Experimentally, self-recognizing $CD8^+$ T-cells from MS patients can elicit an immune response against CNS tissue in naïve mice, demonstrating the ability of this cell subtype to cause CNS pathology (Tsunoda *et al*., 2005). $CD8^+$ T-cells are the most likely candidates for causing axonal damage that leads to demyelination. Roos *et al.* report that both $CD4^+$ and $CD8^+$ T-cells can induce demyelination since depletion of either population leads to myelin breakdown, and that the DA strain of TMEV can damage myelin in both MHC-I and MHC-II-deficient mice (Roos, 2010). However, mice that lack either $CD8^+$ cells or MHC-I have less severe disease outcomes, thus the $CD8^+$ population may cause more damage to axons, impede repair mechanisms, and lead to demyelination (Roos, 2010).

The CNS is considered to be an immunoprivileged site. In infection, however, this is not the case. The cytokine environment created by inflammatory cells determines whether or not the brain will have inflammation and demyelination. $CD4^+$ cells respond to TMEV infection early on. Of the two subtypes of T-helper (T_H) cells, the response mounted against TMEV seems to be T_H1-mediated, or pro-inflammatory. T_H1 cells are polarized by interleukin-12 (IL-12), which is a pro-inflammatory cytokine. $CD4^+$-T_H1 cells will secrete cytokines such as interleukin-2 (IL-2), interferon gamma (IFNγ) and tumor necrosis factor beta (TNFβ). These cytokines are involved in cell-mediated immunity and work to activate macrophages (MΦ) (via IFNγ), recruit lymphpcytes (via TNFβ+IFNγ), cause $CD8^+$ cells to differentiate into cytolytic T-cells (T_{CL}) (via IL-2+IFNγ), and switch IgG to IgG_{2a}, which binds to $F_{C\gamma}$ and binds complement to help in

opsonization (Abbas *et al*., 1996). In MS and EAE, a new subset of T_H cells has also been implicated in inflammation and demyelination. T_H17 cells secrete IL-17 and are induced by IL-6 and transforming growth factor beta (TGFβ), and maintained by IL-23, a cytokine related to IL-12 by its p40 subunit (Aranami and Yamamura, 2008; Fletcher *et al*., 2010); thus, for a long time, the presence of T_H17 cells was unnoticed until 2003, when Cua *et al.* discovered this subgroup of cells (Aranami and Yamamura, 2008). IL-17 attracts neutrophils into the brain, and causes the release of more pro-inflammatory cytokines (Fletcher *et al*., 2010). T_H17 $CD4^+$ cells can induce EAE in naïve mice, thus they are now associated with the pathogenesis of chronic demyelinating disease of the CNS. It is not surprising that this cytokine environment causes damage to CNS tissue as observed in the placebo-treated infected mice.

Estrogens have been shown to induce a switch to a T_H2, or anti-inflammatory environment. E_2 was shown to inhibit T_H1 and T_H17 cell differentiation in the EAE model of MS via interaction with ERα (Lélu *et al*., 2011), which is of significance to this project. Estrogens are known to induce a shift toward T_H2-mediated immunity by influencing T-cells directly via interaction with ERα (Giraud *et al*., 2010), especially during pregnancy (Nicot, 2009).

Theiler's virus has been shown to increase expression of cyclooxygenase-2 (COX-2) in oligodendrocytes and astrocytes. The enzyme cyclooxygenase-2 (COX-2) converts arachidonic acid to prostanoids, which are known to mediate responses during inflammation. Of notable interest is the pro-inflammatory molecule Prostaglandin E2 (PGE2), which is known to induce excitotoxic neuronal death by binding to EP1 receptors. Similar mechanisms are thought to be at play for oligodendrocyte death (Carlson *et al*., 2010). Treatment with E_2 has been shown to protect oligodendrocytes from glutamate excitotoxic cell death by reducing expression of COX-2, which renders them vulnerable to the toxic effects of glutamate (Carlson *et al*., 2010; Molina-Holgado *et al*., 2002), and increasing astrocyte reuptake of glutamate (Spence and Voskuhl, 2012).

The T_H2 cytokine environment is anti-inflammatory and it causes a shift toward humoral immunity. T_H2 cells produce cytokines that help reduce inflammation such as IL-3, 4, 5, 10, and 13. Some of these cells produce TGFβ, but it is produced in other tissues (Abbas *et al*., 1996) and depending on the cytokine milieu, it can induce a shift toward T_H17 or induced regulatory T-cells (iT_{Reg}) (Aranami and Yamamura, 2008). IL-4 causes a shift in IgG subclass to neutralizing (non-complement binding) IgG_1. In B-cells it switches to IgE expression, which helps in mast cell-mediated reactions (response to allergens). IL-3, 4, and 5 cause activation of eosinophils and increase the production of eotaxin to guide them when dealing with helminthes. IL-4 also inhibits IFNγ and prevents MΦ activation, IL-10 inhibits MΦ responses, and TGFβ inhibits activation of other leukocytes. Thus, T_H2-mediated immunity prevents acute and chronic inflammation – including the delayed-type hypersensitivity (DTH) reactions brought about by T_H1 $CD4^+$ cells and limit their responses (Abbas *et al*., 1996).

During classical infection, it is common to initiate T_H1-mediated immunity early and then switch to T_H2 for control and memory functions (Abbas *et al*., 1996). However, during auoimmune chronic inflammation or infection, having T_H1 responses may not be ideal. The switch from T_H1 to T_H2-mediated immunity explains the observations made in the inflammation and demyelination sections of this project.

In addition T_H2 $CD4^+$ cells can induce the shift of uncommitted T-cells into iT_{Reg}s such as T-regulatory-1 (T_R1), T_R3, and $CD8^+T_{Reg}$ via secretion of anti-inflammatory cytokines TGFβ and IL-10, and retinoic acid (RA) (Fletcher *et al*., 2010). Natural T_{Reg}s (nT_{Reg}s) are found in the thymus and they express CD25 and Forkhead box P3 (FoxP3) transcription factor on their cell surface ($CD25^+FoxP3^+$) to elicit regulatory functions (Fletcher *et al*., 2010). It is known that nT_{Reg}s regulate tolerance to self and are important in autoimmunity. In MS patients, increased T_{Reg} activity correlates with symptom remission as the cells try to combat increased inflammation from T_H1/T_H17 cells, and one can speculate that perhaps the relapsing-remitting onset of MS may be related to success of these cells in controlling inflammation, this however is beyond the scope of this project. In the TMEV model, specifically in SJL/J mice, T_{Reg}s are

preferentially activated, and this prevents the virus from being properly cleared from the CNS, which brings us closer to understanding the reason behind the chronic inflammation caused by the virus, and also to understanding MS pathogenesis (Getts *et al*., 2010).

In a recent study by Valor *et al.,* MS pregnant and non-pregnant women were recruited to measure the effects of E_2 on T_{Reg}s (Valor *et al*., 2011). The results of this study showed that E_2 enhances T_{Reg} generation, in accordance to other studies that showed the same (Yates *et al*., 2010), and increases perforin expression (Valor *et al*., 2011). Perforin has been postulated as a mechanism of T_{Reg} *modus operandi*, complete with degranulation as in the granzyme-perforin pathway found in T_{CL}s. It also found that at higher doses, or levels of E_2, such as in pregnancy, T_{Reg} perforin expression is diminished in accordance to the recruitment of T_{Reg}s to the fetal-maternal interface (Valor *et al*., 2011). This novel finding helps explain the reduced levels of inflammation and demyelination in the E_2-treated mice with more accuracy, and aids in the proposal of a mechanism of action for estrogens in the TMEV model of MS.

B-cells and plasma cells in human MS and in TVID have recently received considerable attention. $CD138^+$ cells are commonly attributed the title of mature plasma cells. In the CNS these antibody-secreting cells (ASCs) are part of a secretion system known as intrathecal antibody production (ITAbP) (Pachner *et al*., 2007). ITAbP ASCs are non-existent in normal CNS tissue, but upon infection with TMEV their numbers increase within months of infection and they begin secreting IgG_{2a} class anti-TMEV antibodies to try to eliminate the virus (Pachner *et al*., 2007). Mice infected with the BeAn strain of TMEV showed that the levels of antibody were high in cerebrospinal fluid (CSF), and that the ITAb-producing cells were found around or in close proximity to blood vessels (Pachner *et al*., 2011). However, repeated exposure may result in cross-reaction with myelin components, namely galactocerebroside (Sato *et al*., 2011). In this pro-inflammatory milieu mediated by T_H1 responses, the principal cytokine interferon gamma (IFN-γ) helps promote IgG_{2a} secretion by plasma cells (Dal Canto *et al*., 2000; Nicot, 2009; Peterson *et al*., 1992; Tsunoda *et al*., 2005). Antibody titers measured by

enzyme-linked immunosorbent assay (ELISA) in SJL/J mice infected with TMEV show that IgG_{2a} is preferentially expressed between days 29 and 108 pi. The CNS in these mice is under T_H1-mediated immunity, thus IgG_{2a} production is regulated by IFNγ. In TMEV-resistant C57BL/6 mice, the T_H2 environment regulates IgG_1 production via IL-4 (Miller *et al*., 1995; Peterson *et al*., 1992). In addition, these cells were found to be in locations that parelleled demyelinating lesions, predominantly in ventral white matter areas of the spinal cord (Pachner *et al*., 2011). As mentioned before, E_2 and E_3 are known to switch the T_H1-mediated immunity to T_H2-mediated (Giraud *et al*., 2010; Nicot, 2009). We used a Radio-Immuno Assay (RIA) using protein-A-I^{125}-labeling to measure the amount of TMEV (GD-VII) Antibody in mouse sera. We expected to see a difference between the estrogen-treated groups and placebo-treated group. We did not find significant differences between E_2 and E_3-treated mice at any dilution; however, both groups were significantly different from placebo-treated mice. These results agree with the observations made by Peterson *et al.* as our experiments show that E_2 and E_3 both cause a shift to T_H2-mediated immunity and IgG_1, while placebo-treated mice stay on the T_H1-mediated milieu and secrete IgG_{2a} (Peterson *et al*., 1992).

5. CONCLUSION AND FUTURE DIRECTIONS

Our study concludes that the use of estrogens as potential therapeutic agents in a murine model of multiple sclerosis is plausible in early disease or as a preventive treatment (Vegeto *et al*., 2008). The use of estrogens, in particular 17-β-estradiol ameliorated clinical symptoms, reduced signs of inflammation and demyelination, and reduced TMEV antibody counts. This effect is supported by observations made by other research groups. Treatment with estriol is not helpful in ameliorating symptoms. Though it seems to reduce inflammation mildly and diminish TMEV antibody counts, it does not seem to help with demyelination. Though these results are in disagreement with other experimental models of MS, there may be differences in the pathogenic mechanisms of TMEV that can account for our findings. Figure 5.1 presents a proposed mechanism for the beneficial effects of estradiol on TMEV.

Future studies will need to explore the populations of T_H-cells present in the lesions, explore the cytokine environments present in the different treatment groups and confirm the role of T_{Reg}s in this model. Studies of the brain in TMEV have not been conducted, thus it would be important to look at the brains in the different treatment groups and assess inflammation and demyelination to create a neuroanatomical model for the pathogenesis of Theiler's Murine Encephalomyelitis Virus. In addition further analysis of cytokine profiles in the experimental groups may provide potential mechanisms of action of estrogens in modulating the immune response and protecting inflammatory demyelination. Studies using hormones such as progesterone for the treatment of TVID may also be in order. Finally, to assess whether hormone treatments may be effective in males, studies with male mice should be carried out.

Figure 5.1 Proposed mechanism of action of estradiol in TVID.
We propose that estrogens, in particular 17-β-estradiol (E_2), reduce inflammation and demyelination via interaction with estrogen receptors (ERs) in cells of the CNS. The result is a decrease in clinical scores and severity of disease.

A) E_2 induces a switch from a T_H1 (pro-inflammatory) to a T_H2 (anti-inflammatory) cytokine environment. Interleukin (IL)-4, IL-5, IL-10, IL-13, and TGFβ are cytokines produced in this environment and they inhibit macrophage activity and modulate T-cell responses
B) E_2 prevents the pro-inflammatory p65 transcription factor of the (NF-κB family) from entering the nucleus to promote transcription of inflammatory genes.
C) E_2 restores the impermeability of the blood-brain barrier (BBB) following ovariectomy and prevents leukocyte infiltration into the CNS.
D) E_2 can inhibit viral replication of TMEV which prevents direct lysis or infection of other cells.
E) E_2 interacts with ERs in astrocytes inducing the reuptake of glutamate (Glu) reducing its excitotoxic effects. It also reduces the expression of COX2 in astrocytes reducing the production of prostanoids
F) COX2 expression in oligodendrocyte has been associated with cell death. E_2 inhibits COX2 production in Oligodendrocytes, preventing death and demyelination.
G) E_2 induces a switch in immunoglobulin (Ig) class in both B-cells and plasma cells. IgG_1 has been associated with a T_H2 response and less myelin damage due to antibodies.
H) E_2 induces T_{Reg} generation and perforin production, which may the mechanism by which these cells regulate autoimmune responses

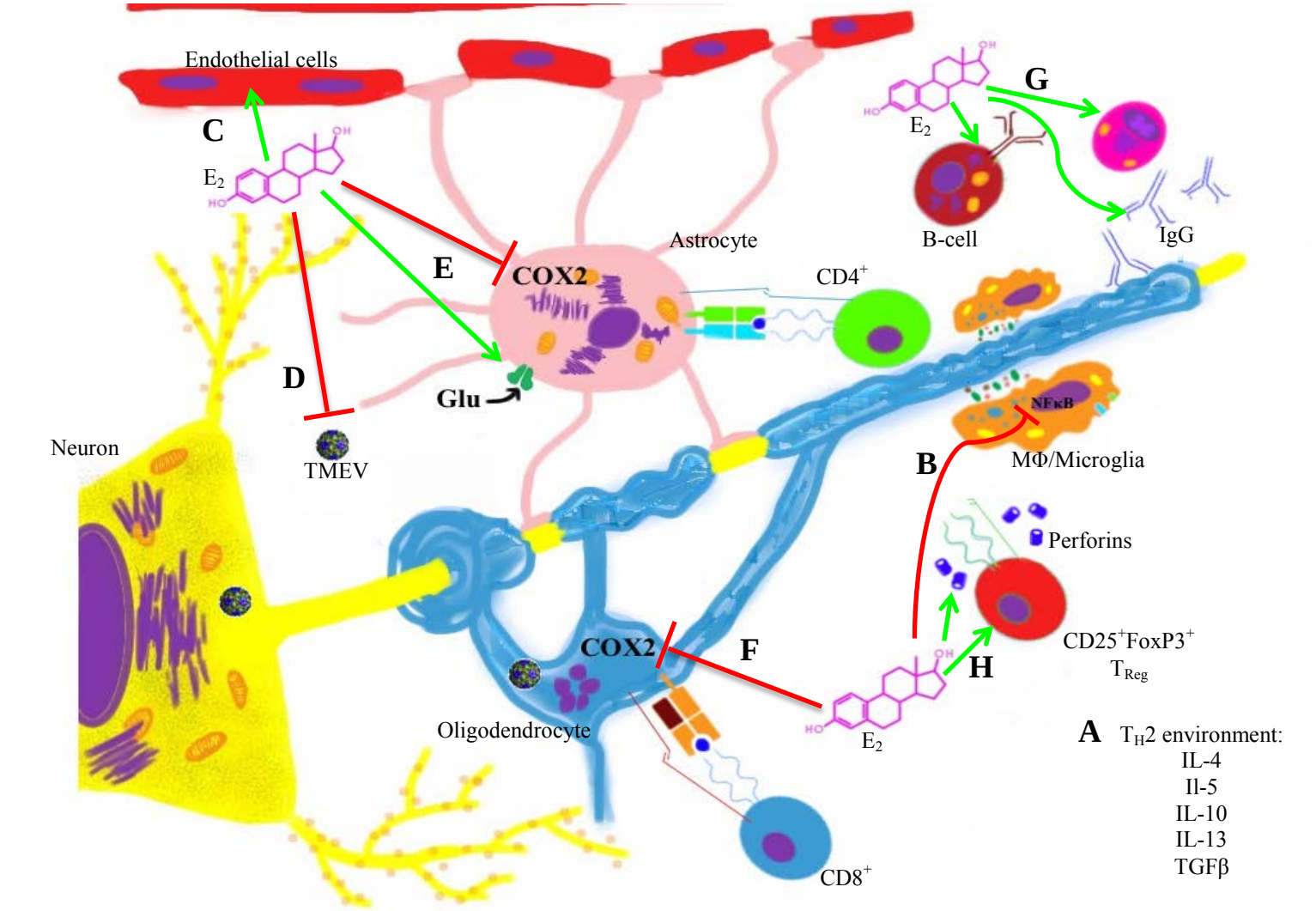
Endothelial cells
C
E2
E
COX2
Astrocyte
CD4+
D
Glu
TMEV
Neuron
G
E2
B-cell
IgG
NFκB
B
MΦ/Microglia
Perforins
CD25+FoxP3+
TReg
COX2
F
H
E2
Oligodendrocyte
CD8+
A TH2 environment:
IL-4
Il-5
IL-10
IL-13
TGFβ

REFERENCES

Abbas, A.K., Murphy, K.M., Sher, A., 1996. Functional diversity of helper T lymphocytes. Nature. 383, 787-793.

Abramsky, O., 1994. Pregnancy and multiple sclerosis. Ann Neurol. 36, S38-41.

Alonso, A., Jick, S., Olek, M.J., Ascherio, A., Jick, H., Hernan, M.A., 2005. Recent use of oral contraceptives and the risk of multiple sclerosis. Arch Neurol. 62, 1362-1365

Aranami, T., Yamamura, T., 2008. Th17 Cells and autoimmune encephalomyelitis (EAE/MS). Allergology International 57, 115-120.

Bebo, B.F., Fyfe-Johnson, A., Adlard, K., Beam, A.G., Vandenbark, A.A., Offner, H., 2001. Low-dose estrogen therapy ameliorates experimental autoimmune encephalomyelitis in two different inbred mouse strains. Journal of Immunology 166, 2080-2089.

Blakemore, W.F., Welsh, C.J., Tonks, P., Nash, A.A., 1988. Observations on demyelinating lesions induced by Theiler's virus in CBA mice. Acta Neuropathol 76, 581-589.

Calabrese, M., Filippi, M., Rovaris, M., Mattisi, I., Bernardi, V., Atzori, M., Favaretto, A., Barachino, L., Rinaldi, L., Romualdi, C., Perini, P., Gallo, P., 2008. Morphology and evolution of cortical lesions in multiple sclerosis. A longitudinal MRI study. Neuroimage 42, 1324-1328.

Campbell, T., Meagher, M.W., Sieve, A., Scott, B., Storts, R., Welsh, T.H., Welsh, C.J., 2001. The effects of restraint stress on the neuropathogenesis of Theiler's virus infection: I. Acute disease. Brain, Behavior, and Immunity 15, 235-254.

Carlson, C.a.R., Stephen C, 2006. Multiple sclerosis. Microsoft® Encarta® 2006 [DVD], Microsoft Corporation.

Carlson, N.G., Rojas, M.A., Redd, J.W., Tang, P., Wood, B., Hill, K.E., Rose, J.W., 2010. Cyclooxgenase-2 expression in oligodendrocytes increases sensitivity to excitotoxic death. Journal of Neuroinflammation 7, 25-35.

Chastain, E.M.L., Duncan, D.A.S., Rodgers, J.M., Miller, S.D., 2011. The role of antigen presenting cells in multiple sclerosis. Biochimica et Biophysica Acta 1812, 265-274.

Cipolla, M., Godfrey, J., Wiegman, M., 2009. The effect of ovariectomy and estrogen on penetrating brain arterioles and blood-brain barrier permeability. Microcirculation 16, 685-693.

Confavreux, C., Hutchinson, M., Hours, M.M., Cortinovis-Tourniaire, P., Moreau, T., 1998. Rate of pregnancy-related relapse in multiple sclerosis. New England Journal of Medicine 339, 285-291.

Cottrell, D.A., Kremenchutzky, M., Rice, G.P.A., Koopman, W.J., Hader, W., Baskerville, J., Ebers, G.C., 1999. The natural history of multiple sclerosis:a geographically based study. Brain 122, 625-639.

Dal Canto, M.C., Calenoff, M.A., Miller, S.D., Vanderlugt, C.L., 2000. Lymphocytes from mice chronically infected with Theiler's murine encephalomyelitis virus produce demyelination of organotypic cultures after stimulation with the major encephalitogenic epitope of myelin proteolipid protein. Epitope spreading in TMEV infection has functional activity. Journal of Neuroimmunology 104, 79-84.

Fletcher, J.M., Lalor, S.J., Sweeney, C.M., Tubridy, N., Mills, K.H.G., 2010. T cells in multiple sclerosis and experimental autoimmune encephalomyelitis. Clinical and Experimental Immunology 162, 1-11.

Fuller, A.C., Kang, B., Kang, H.K., Yahikozowa, H., Dal Canto, M.C., Kim, B.S., 2005. Gender bias in Theiler's virus-induced demyelinating disease correlates with the level of antiviral immune responses. Journal of Immunology 175, 3955-3963.

Garay, L., Deniselle, M.C.G., Lima, A., Roig, P., De Nicola, A.F., 2007. Effects of progesterone in the spinal cord of a mouse model of multiple sclerosis. J Steroid Biochem Mol Biol 107, 228-237.

Gasperini, C., Ruggieri, S., Pozzilli, C., 2010. Emerging oral treatments in multiple sclerosis - clinical utility of cladribine tablets. Ther Clin Risk Manag 6, 391-399.

Getts, M.T., Richards, M.H., Miller, S.D., 2010. A critical role for virus-specific CD8+ CTLs in protection from Theiler's virus-induced demyelination in disease-susceptible SJL mice. Virology 402, 102-111.

Ghadge, G.D., Wollmann, R., Baida, G., Traka, M., Roos, R.P., 2011. The L-coding region of the DA strain of Theiler's murine encephalomyelitis virus causes dysfunction and death of myelin-synthesizing cells. Journal of Virology 85, 9377-9384.

Giraud, S.N., Caron, C.M., Pham-Dinh, D., Kitabgi, P., Nicot, A.B., 2010. Estradiol inhibits ongoing autoimmune neuroinflammation and NFκB-dependent CCL2

expression in reactive astrocytes. Proceedings of the National Academy of Sciences of the United States of America 107, 8416-8421.

Gold, R., Wolinsky, J.S., 2011. Pathophysiology of multiple sclerosis and the place of teriflunomide. Acta Neurologica Scandinavica 124, 75-84.

Gold, S.M., Voskuhl, R.R., 2009. Estrogen and testosterone therapies in multiple sclerosis. In: Verhaagen, J., Hol, E.M., Huitenga, I., Wijnholds, J., Bergen, A.B., Boer, G.J., Dick, F.S. (Eds.), Progress in Brain Research, Elsevier, New York, pp. 239-251.

Goodin, D.S., 2009. The causal cascade to multiple sclerosis: A model for MS pathogenesis. PLoS One 4, e4565.

Kappel, C.A., Melvold, R.W., Kim, B.S., 1990. Influence of sex on susceptibility in the Theiler's murine encephalomyelitis virus model for multiple sclerosis. Journal of Neuroimmunology 29, 15-19.

Kipp, M., Beyer, C., 2009. Impact of sex steroids on neuroinflammatory processes and experimental multiple sclerosis. Frontiers in Neuroendocrinology 30, 188-200.

Lélu, K., Laffont, S., Delpy, L., Paulet, P.-E., Périnat, T., Tschanz, S.A., Pelletier, L., Engelhardt, B., Guéry, J.-C., 2011. Estrogen receptor- α signaling in T-lymphocytes is required for estradiol-mediated inhibition of Th1 and Th17 cell differentiation and protection against experimental autoimmune encephalomyelitis. Journal of Immunology 187, 2386-2393.

Libbey, J., Fujinami, R., 2010. Potential triggers of MS molecular basis of multiple sclerosis. In: Martin, R., Lutterotti, A. (Eds.), Results and Problems in Cell Differentiation, Springer Berlin, pp. 21-42.

Meagher, M., Johnson, R., Young, E., Vichaya, E., Lunt, S., Hardin, E., Connor, M., Welsh, C.J.R., 2007. Interleukin-6 as a mechanism for the adverse effects of social stress on acute Theiler's virus infection. Brain, Behavior, and Immunity 21, 1083-1095.

Mendez-Fernandez, Y.V., Hansen, M.J., Rodriguez, M., Pease, L.R., 2005. Anatomical and cellular requirements for the activation and migration of virus-specific CD8+ T-cells to the brain during Theiler's virus infection. Journal of Virology 79, 3063-3070.

Miller, S.D., Katz-Levy, Y., Neville, K.L., Vanderlugt, C.L., 2001. Virus-induced autoimmunity: Epitope spreading to myelin autoepitopes in Theiler's virus infection of the central nervous system. In: Michael J. Buchmeier, I.L.C. (Ed.), Advances in Virus Research, Academic Press, New York, pp. 199-217.

Miller, S.D., McRae, B.L., Vanderlugt, C.L., Nikcevich, K.M., Pope, J.G., Pope, L., Karpus, W.J., 1995. Evolution of the T-cell repertoire during the course of experimental immune-mediated demyelinating diseases. Immunol Rev 144, 225-244.

Molina-Holgado, E., Arévalo-Martín, A., Ortiz, S., Vela, J.M., Guaza, C., 2002. Theiler's virus infection induces the expression of cyclooxygenase-2 in murine astrocytes: inhibition by the anti-inflammatory cytokines interleukin-4 and interleukin-10. Neuroscience Letters 324, 237-241.

Nicot, A., 2009. Gender and sex hormones in multiple sclerosis pathology and therapy. Frontiers in Bioscience 14, 4477–4515.

Njenga, M.K., Asakura, K., Hunter, S.F., Wettstein, P., Pease, L.R., Rodriguez, M., 1997. The immune system preferentially clears Theiler's virus from the gray matter of the central nervous system. Journal of Virology 71, 8592-8601.

Oleszak, E.L., Chang, J.R., Friedman, H., Katsetos, C.D., Platsoucas, C.D., 2004. Theiler's virus infection: A model for multiple sclerosis. Clinical Microbiology Reviews 17, 174-207.

Olsson, T., Hillert, J., 2008. The genetics of multiple sclerosis and its experimental models. Current Opinion in Neurology 21, 255-260.

Owens, G., Gilden, D., Burgoon, M., Yu, X., Bennett, J., 2011. Viruses and multiple sclerosis. The Neuroscientist 17, 659-676.

Pachner, A.R., Brady, J., Narayan, K., 2007. Antibody-secreting cells in the central nervous system in an animal model of MS: Phenotype, association with disability, and in vitro production of antibody. Journal of Neuroimmunology 190, 112-120.

Pachner, A.R., Li, L., Lagunoff, D., 2011. Plasma cells in the central nervous system in the Theiler's virus model of multiple sclerosis. Journal of Neuroimmunology 232, 35-40.

Palaszynski, K.M., Liu, H., Loo, K.K., Voskuhl, R.R., 2004. Estriol treatment ameliorates disease in males with experimental autoimmune encephalomyelitis: implications for multiple sclerosis. Journal of Neuroimmunology 149, 84-89.

Peterson, J.D., Waltenbaugh, C., Miller, S.D., 1992. IgG subclass responses to Theiler's murine encephalomyelitis virus infection and immunization suggest a dominant role for Th1 cells in susceptible mouse strains. Immunology 75, 652-658.

Rinta, S., Airas, L., Elovaara, I., 2010. Is the modulatory effect of pregnancy in multiple sclerosis associated with changes in blood apoptotic molecules? Acta Neurologica Scandinavica 122, 168-174.

Roos, R.P., 2010. Pathogenesis of Theiler's murine encephalomyelitis virus-induced disease. Clinical and Experimental Neuroimmunology 1, 70-78.

Roussarie, J.-P., Ruffié, C., Edgar, J.M., Griffiths, I., Brahic, M., 2007. Axon myelin transfer of a non-enveloped virus. PLoS One 2, e1331.

Sato, F., Tanaka, H., Hasanovic, F., Tsunoda, I., 2011. Theiler's virus infection: Pathophysiology of demyelination and neurodegeneration. Pathophysiology 18, 31-41.

Selvamani, A., Sohrabji, F., 2010. Reproductive age modulates the impact of focal ischemia on the forebrain as well as the effects of estrogen treatment in female rats. Neurobiol Aging 31, 1618-1628.

Shaikh, A.A., 1971. Estrone and estradiol levels in the ovarian venous blood from rats during the estrous cycle and pregnancy. Biol Reprod 5, 297-307.

Sicotte, N.L., Liva, S.M., Klutch, R., Pfeiffer, P., Bouvier, S., Odesa, S., Wu, T.C.J., Voskuhl, R.R., 2002. Treatment of multiple sclerosis with the pregnancy hormone estriol. Annals of Neurology 52, 421-428.

Sieve, A.N., Steelman, A.J., Young, C.R., Storts, R., Welsh, T.H., Welsh, C.J., Meagher, M.W., 2006. Sex-dependent effects of chronic restraint stress during early Theiler's virus infection on the subsequent demyelinating disease in CBA mice. Journal of Neuroimmunology 177, 46-62.

Sieve, A.N., Steelman, A.J., Young, C.R., Storts, R., Welsh, T.H., Welsh, C.J.R., Meagher, M.W., 2004. Chronic restraint stress during early Theiler's virus infection exacerbates the subsequent demyelinating disease in SJL mice. Journal of Neuroimmunology 155, 103-118.

Smith, R., Studd, J.W., 1992. A pilot study of the effect upon multiple sclerosis of the menopause, hormone replacement therapy and the menstrual cycle. Journal of the Royal Society of Medicine 85, 612-613.

Smith-Bouvier, D.L., Divekar, A.A., Sasidhar, M., Du, S., Tiwari-Woodruff, S.K., King, J.K., Arnold, A.P., Singh, R.R., Voskuhl, R.R., 2008. A role for sex chromosome complement in the female bias in autoimmune disease. Journal of Experimental Medicine 2008 205, 1099-1108. Epub 2008 Apr 1028.

Soldan, S., Alvarez Retuerto, A., Sicotte, N., Voskuhl, R., 2003. Immune modulation in multiple sclerosis patients treated with the pregnancy hormone estriol. Journal of Immunology 171, 6267-6274.

Spence, R.D., Hamby, M.E., Umeda, E., Itoh, N., Du, S., Wisdom, A.J., Cao, Y., Bondar, G., Lam, J., Ao, Y., Sandoval, F., Suriany, S., Sofroniew, M.V., Voskuhl, R.R., 2011. Neuroprotection mediated through estrogen receptor- α in astrocytes. Proceedings of the National Academy of Sciences 108, 8867-8872.

Spence, R.D., Voskuhl, R.R., 2012. Neuroprotective effects of estrogens and androgens in CNS inflammation and neurodegeneration. Frontiers in Neuroendocrinology 33, 105-115.

Stadelmann, C., Albert, M., Wegner, C., Brck, W., 2008. Cortical pathology in multiple sclerosis. Current Opinion in Neurology 21, 229-234.

Stuart, M., Bergstrom, L., 2011. Pregnancy and multiple sclerosis. Journal of Midwifery & Women's Health 56, 41-47.

Tiwari-Woodruff, S., Voskuhl, R., 2009. Neuroprotective and anti-inflammatory effects of estrogen receptor ligand treatment in mice. Journal of the Neurological Sciences 286, 81-85.

Tsunoda, I., Kuang, L.-Q., Kobayashi Warren, M., Fujinami, R., 2005. Central nervous system pathology caused by autoreactive CD8+ T-cell clones following virus infection. Journal of Virology 79, 14640-14646.

Valor, L., Teijeiro, R., Aristimuño, C., Faure, F., Alonso, B., de Andres, C., Tejera, M., Lopez-Lazareno, N., Fernandez-Cruz, E., Sanchez-Ramon, S., 2011. Estradiol-dependent perforin expression by human regulatory T-cells. Eur J Clin Invest 41, 357-364.

Vegeto, E., Benedusi, V., Maggi, A., 2008. Estrogen anti-inflammatory activity in brain: A therapeutic opportunity for menopause and neurodegenerative diseases. Frontiers in Neuroendocrinology 29, 507-519.

Voskuhl, R., 2003. Hormone-based therapies in MS. The International MS Journal 10, 60-66.

Voskuhl, R.R., Palaszynski, K., 2001. Sex hormones in experimental autoimmune encephalomyelitis: Implications for multiple sclerosis. The Neuroscientist 7, 258-270.

Wang, C., Dehghani, B., Li, Y., Kaler, L.J., Vandenbark, A.A., Offner, H., 2009. Oestrogen modulates experimental autoimmune encephalomyelitis and interleukin-17 production via programmed death 1. Immunology 126, 329-335.

Weil, A., 1928. A rapid method for staining myelin sheaths. Arch Neurol Psychiatry 20, 392-393.

Welsh, C.J., Tonks, P., Nash, A.A., Blakemore, W.F., 1987. The effect of L3T4 T-cell depletion on the pathogenesis of Theiler's murine encephalomyelitis virus infection in CBA mice. The Journal of General Virology 68 (Pt 6), 1659-1667.

Whitacre, C.C., 2001. Sex differences in autoimmune disease. Nat Immunol. 2, 777-780.

Yates, M.A., Li, Y., Chlebeck, P., Proctor, T., Vandenbark, A.A., Offner, H., 2010. Progesterone treatment reduces disease severity and increases IL-10 in experimental autoimmune encephalomyelitis. Journal of Neuroimmunology 220, 136-139.

Young, E.E., Sieve, A.N., Vichaya, E.G., Carcoba, L.M., Young, C.R., Ambrus, A., Storts, R., Welsh, C.J.R., Meagher, M.W., 2010. Chronic restraint stress during early Theiler's virus infection exacerbates the subsequent demyelinating disease in SJL mice: II. CNS disease severity. Journal of Neuroimmunology 220, 79-89.

VITA

Name: Francisco Pascual Gomez

Address: c/o Dr. Jane Welsh
Department of Veterinary Integrative Biosciences,
College of Veterinary Medicine and Biomedical Science.
Mail Stop 4458
College Station, TX 77843-4458

Email Address: FPGomez2515@yahoo.com

Education: B.S. Biomedical Sciences, *cum laude*, Texas A&M University, 2009
M.S. Biomedical Sciences, Texas A&M University, 2012
Admitted to Texas A&M Health Science Center College of Medicine, Class of 2016

Awards:

- Second place graduate poster presentation winner at the 4th Annual Faculty of Neuroscience (FNS) Symposium – April 20, 2012
- Recipient of the Margaret and Charles Plumb Endowed Scholarship (Academic year 2011-2012)
- Recipient of the Patricia A Ward College of Medicine Scholarship (Academic year 2010-2011)
- College of Veterinary Medicine and Biomedical Science Regents' Graduate Fellowship recipient (Academic year 2009-2010)